LBB EVALUATION OF THE CORE FLOOD AND LOW PRESSURE INJECTION/ DECAY HEAT REMOVAL PIPING SYSTEMS FOR OCONEE UNIT 3

FRA-ANP Document No. 77- 5038568-00
February 2004

Prepared for: Duke Power Co.

Prepared by:
AD Nana
HP Gunawardane

(See the following page for document signatures.)

Framatome ANP, Inc.
An AREVA and Siemens Company
3315 Old Forest Road
P.O. Box 10935
Lynchburg, VA 24506-0935

Signatures:

Prepared by:

2/26/04
AD Nana
Materials and Structural Analysis Unit

2/26/04
HP Gunawardane
Materials and Structural Analysis Unit

Reviewed by:

2/26/04
CJ McGaughy
Materials and Structural Analysis Unit

for S. Fyfitch 2/27/04
S Fyfitch
Materials and Structural Analysis Unit

2/26/04
DE Killian
Materials and Structural Analysis Unit

Approved by:

2/27/2004
AD McKim
Manager,
Materials and Structural Analysis Unit

EXECUTIVE SUMMARY

On October 27, 1987, the Federal Register published a modification to 10 CFR 50, General Design Criterion 4 (GDC 4). The modification to GDC 4 allows exclusion from the design basis of dynamic effects associated with high energy pipe rupture by application of leak-before-break technology. High energy piping is defined in GDC 4 as those systems having pressures exceeding 275 psig or temperatures exceeding 200°F.

This report documents the application of leak-before-break (LBB) technology to portions of the high energy piping of the core flood (CF) and low pressure injection/decay heat removal (LPI/DHR) piping systems (referred to as train "A" and train "B') for Oconee Unit 3. The existing LPI/DHR lines that connect to the CF piping system are planned to receive modifications during the Fall of 2004. The modifications involve installing check valves, flow orifices and cross tie piping between trains "A" and "B."

The high energy piping systems included in this report are the 14 inch CF line connecting the core flood tank with the reactor vessel and a very small portion of the 10 inch LPI/DHR line (65-inch or less in length) that connects from the valve to the ninety-degree tee-fitting with the CF line piping. There are two of these systems at Oconee Unit 3. The following analyses are detailed:

- The piping systems included in this report are reviewed against limiting criteria specified in General Design Criterion 4 (GDC 4) of 10 CFR 50, S.R.P 3.6.3 and NUREG-1061 to determine if LBB is applicable.

- As a result of PWSCC concerns of the Alloy 82/182 weld between the core flood nozzle at the RV and the safe-end piping, this weld location at both train "A" and train "B" of the CF piping is excluded from evaluation for LBB. The Alloy 82/182 welds at the A & B Core Flood Tanks are included, since PWSCC concerns are not applicable due to the low temperature of the fluid within the tank and adjacent piping.

- The mechanical properties of the base metal materials of the piping systems are obtained through review of the Certified Material Test Reports (CMTRs) and applicable experimental data.

- Normal and faulted loads from the latest I&E Bulletin 79-14 analysis are used to calculate the highest stress locations enveloped over both the CF piping systems included in the scope of this report.

- The leak detection systems used in the plants are reviewed to demonstrate that a 1-gallon per minute leak can be identified within one hour. A factor of 10 is applied to this value giving a leakage size crack (LSC) corresponding to leak rate of 10 gallons per minute as required by S.R.P. 3.6.3.

- The crack opening area is determined using the GE/EPRI method for a given circumferential crack and the Paris-Tada method for a given longitudinal crack based on normal operating loads. This analysis uses normal operating loads and normal operating fluid conditions to determine the LSC; i.e., the crack that gives a leak flow rate of 10 gpm.

- S.R.P. 3.6.3 requires that the critical crack length (CCL) have a margin of 2.0 against the LSC when using the absolute sum method of combining faulted loads. The required margin is demonstrated through the tearing instability analysis method using a J versus T diagram.

The current analysis does not include the Alloy 82/182 weld regions between the reactor vessel (RV) core flood nozzle and the safe-end due to PWSCC issues. However, the rest of the CF piping was evaluated for the application of LBB. The margin of 10 on leakage detection, the margin of 2.0 on postulated crack size, and the margin of 1.0 on loads combined by the absolute sum method as required by S.R.P. 3.6.3 are demonstrated. Therefore, the use of leak-before-break technology to eliminate the dynamic effects of postulated pipe breaks in these systems is justified.

RECORD OF REVISIONS

Revision	Affected Pages	Description	Date
0	All	Original release	02/2004

TABLE OF CONTENTS

LIST OF FIGURES

LIST OF TABLES

1. SCOPE

The scope of this leak-before-break (LBB) analysis for the Oconee Unit 3 station includes high energy piping systems that have postulated high energy line break locations in the current design. Oconee Unit 3 contains two of these systems (referred to as train "A" and train "B"). The piping system included in this evaluation primarily contains the high energy Core Flooding (CF) System. It also includes a very small portion of the Low Pressure Injection/Decay Heat Removal System (LPI/DHR). The CF and LPI/DHR subsystems are discussed below.

Core Flooding System (CF)

The core flooding system is used during the postulated loss of coolant accident (LOCA). It acts as part of the emergency core cooling system (ECCS) by providing a sufficient volume of coolant water to cover the core in the case of a complete loss of liquid in the RV. The CF system maintains pressure through use of a nitrogen cover in the core flood tank.

Low Pressure Injection/Decay Heat Removal System (LPI/DHR)

The LPI/DHR system is used during the final stages of normal plant cooldown when heat removal by the main steam system is no longer practical. The LPI/DHR system removes heat from the reactor coolant system and transfers it to the low pressure service water system. The system is also used during the initial stages of plant heatup.

The LPI/DHR system is also used during the postulated loss of coolant accident (LOCA). It acts as part of the emergency core cooling system (ECCS) by providing a low pressure, high volume water source to the reactor coolant system during the injection and recirculation phases.

During normal "at-power" operation, the LPI/DHR system within containment maintains pressure from three different sources. The three sources are the RCS, the CF system and the borated water storage tank (BWST).

The planned addition of a cross tie between train "A" and train "B" (planned for Fall 2004) includes the installation of check valves and flow orifices (one for each train) near the junction of the LPI system with the CF line as illustrated in Figure 1-3. All piping and other installations between the new check valve and the LPI system building penetration, as well as the new cross tie piping, are not included in this analysis.

Piping Within Scope

Isometric drawings of the piping systems included in this analysis are shown in Figures 1-1 and 1-2. These drawings represent the as-analyzed pipe routings for Oconee Unit 3 planned for the Fall 2004 outage. The schematic view of Figure 1-3 also illustrates the new cross tie between Trains A and B. While the figure depicts Unit 1, it is representative of Unit 3 in that the difference between the Units is that all components in Unit 3 are preceded by the Unit number (3). For example, the new check valves that are installed in Unit 3 are named 3LP-176 and 3LP-177. In Unit 1, these check valves are named 1LP-176 and 1LP-177.

The portion of the figure enclosed in dashed lines is the piping analyzed for LBB. Table 1-1 provides the piping materials, pipe sizes, and normal operating fluid parameters for the CF and LPI/DHR piping systems within the LBB scope. The line designations shown in Table 1-1 and on Figures 1-1 and 1-2 indicate the Oconee Unit number, the pipe outside diameter (10 or 14), the pipe schedule (30 or 140), and a breakpoint identifier which is based on pipe size and operating parameters (temperature and pressure).

The high energy CF piping system primarily consists of the 14 inch CF line connecting the core flood tank with the reactor vessel. It includes a portion of the 10 inch LPI/DHR line that connects from the valve to the ninety-degree tee-fitting with the CF line piping. There are two of these systems (train "A" and train "B") at Oconee Unit 3. As a result of PWSCC concerns, the Alloy 82/182 weld between the reactor vessel CF nozzle and the safe-end is not within the LBB scope. The Alloy 82/182 welds at the two core flood tanks are included, since PWSCC is not a concern at this location, due to the low operating temperatures.

Table 1-1 Line Designations

Line Designation	Outside Diameter (in)	Thickness (in)	ASTM Material Spec	Operating Pressure (psig)	Operating Temperature (°F)
3A-14030-1	14.00	0.375	A 358 Cl. 1, Gr. TP304	625	125
3A-14140-2	14.00	1.250	A 376 Gr. TP304H	625	125
3A-14140-3	14.00	1.250	A 376 Gr. TP316H	2200	557
3A-10140-5	10.75	1.000	A 376 Gr. TP304H	625	125
3B-14030-1	14.00	0.375	A 358 Cl. 1, Gr. TP304	625	125
3B-14140-2	14.00	1.250	A 376 Gr. TP304H	625	125
3B-14140-3	14.00	1.250	A 376 Gr. TP316H	2200	557
3B-10140-5	10.75	1.000	A 376 Gr. TP304H	625	125

Figure 1-1 Isometric View of Oconee Unit 3 - Train A CF/LPI/DHR Piping System

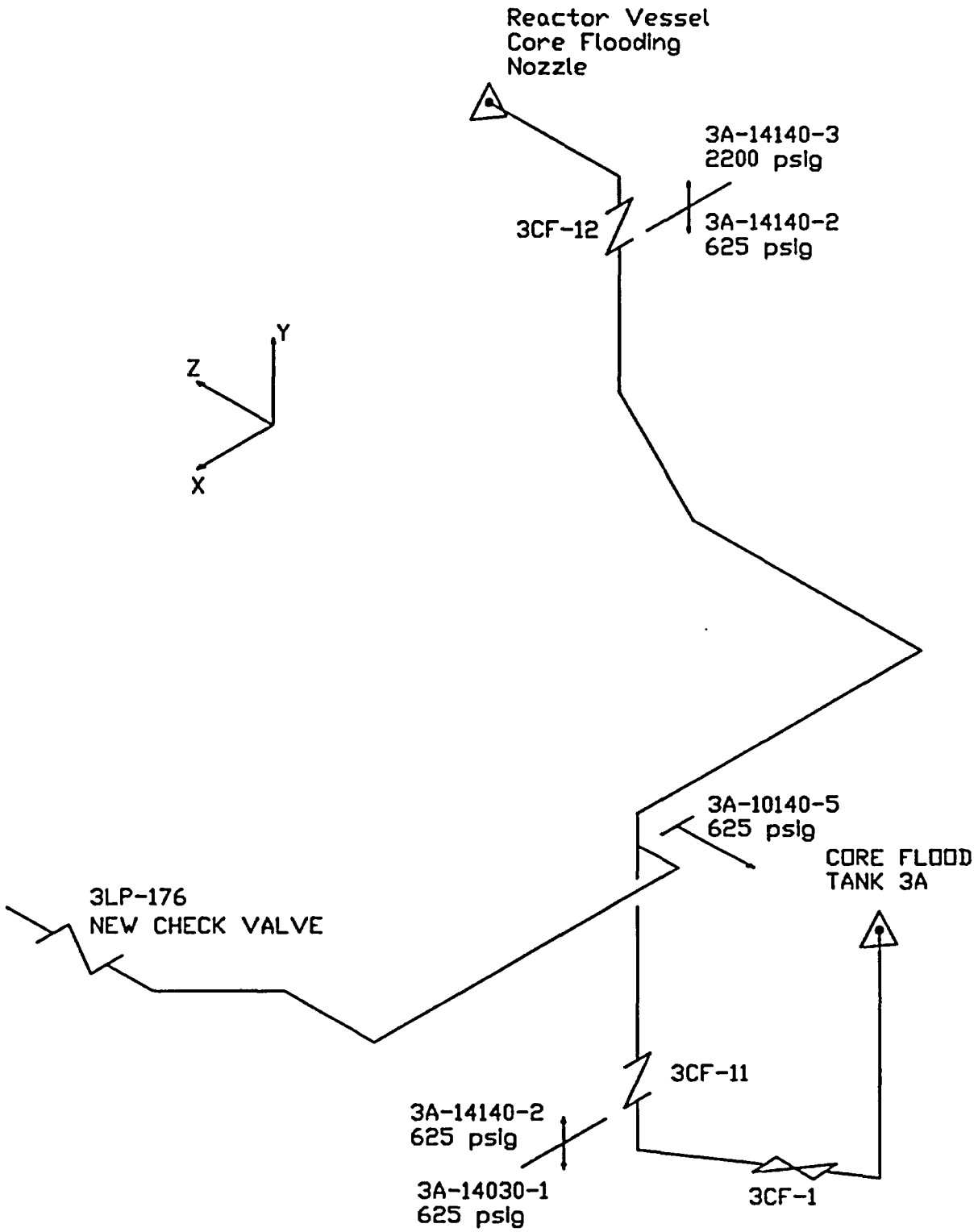

AREVA

Figure 1-2 Isometric View of Oconee Unit 3 - Train B CF/LPI/DHR Piping System

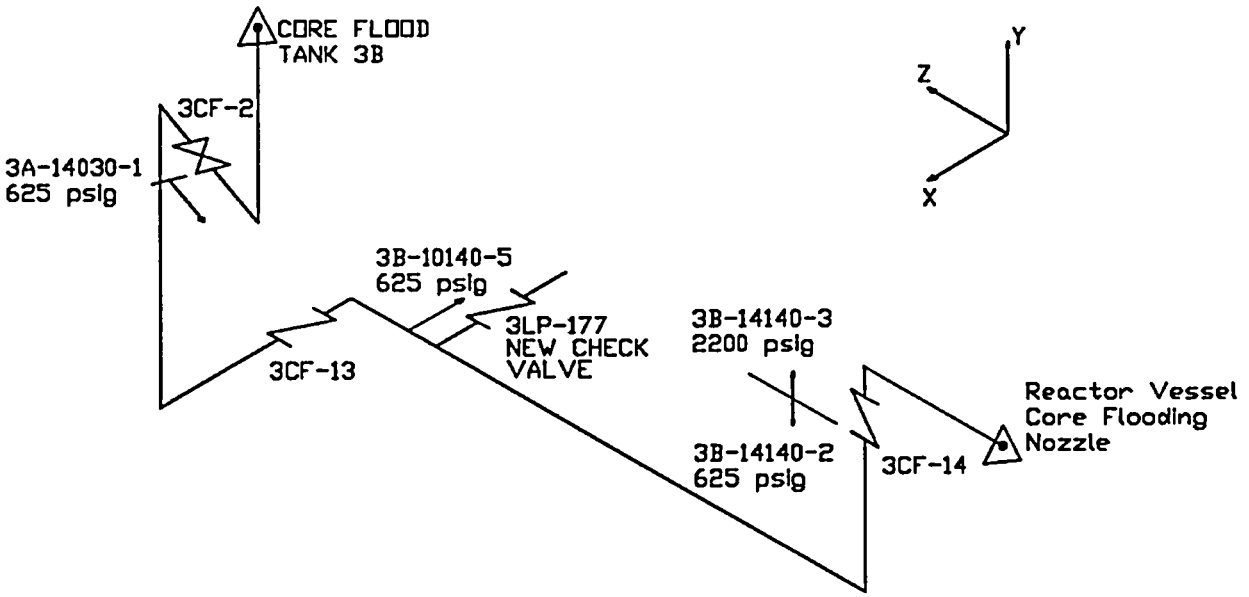

AREVA

Figure 1-3 Schematic View of Oconee Unit 1[1] with Cross Tie

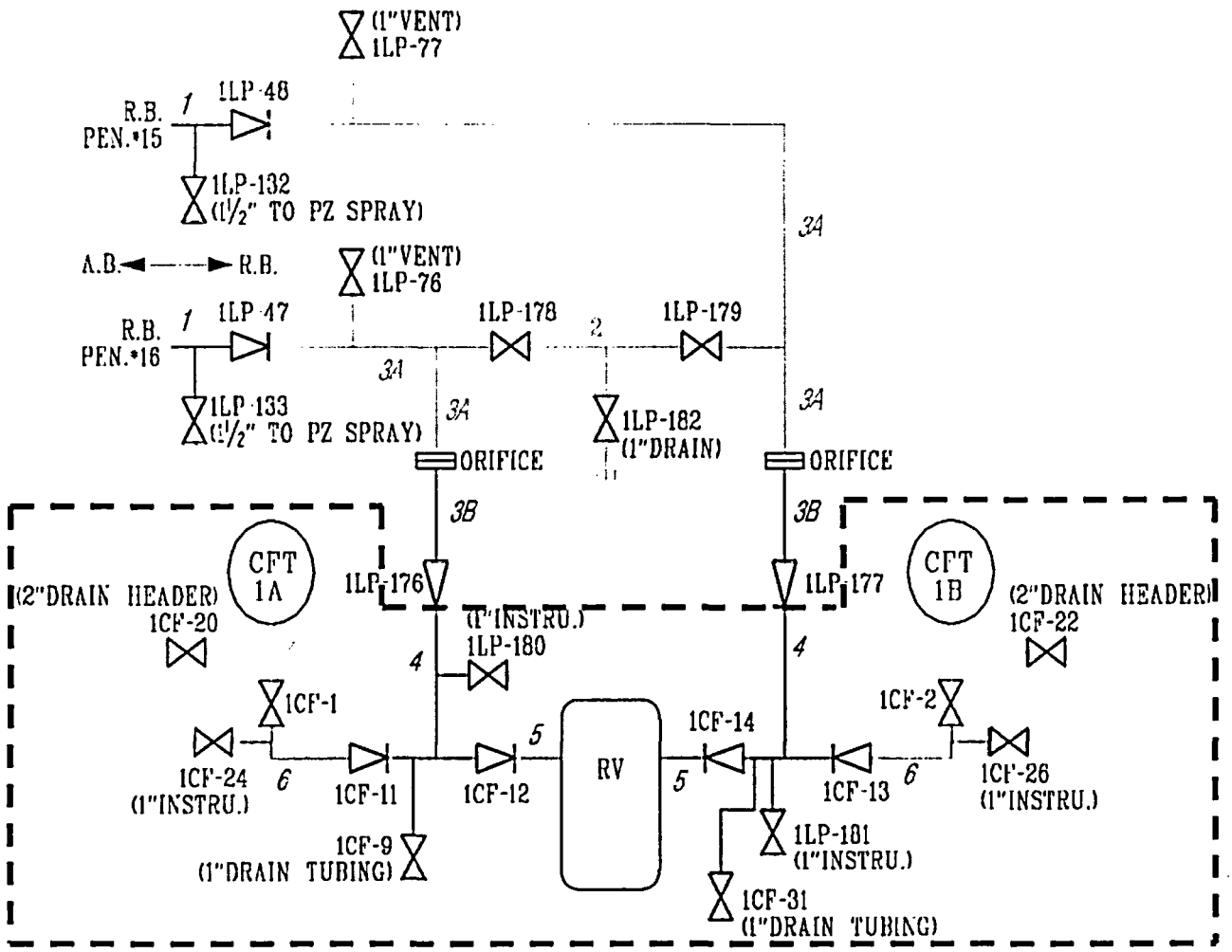

[1] Representative of Unit 3

AREVA

2. APPLICABILITY OF LBB TO CF AND LPI/DHR PIPING SYSTEMS

NUREG-1061 (Reference 1) provides recommendations for application of the LBB approach in the NRC licensing process. In Volume 3 of NUREG-1061, Section 5.1 provides six limitations to be applied to the mechanistic evaluation of pipe breaks in high-energy fluid system piping:

- For specifying design criteria for emergency core coolant systems, containments, and other engineered safety features, loss of coolant shall be assumed in accordance with existing regulations. The evaluation of environmental effects should be considered case-by-case.

- The LBB approach should not be considered applicable to high-energy fluid system piping, or portions thereof, that operating experience has indicated particular susceptibility to failure from the effects of corrosion (e.g., intergranular stress corrosion cracking), water hammer, or low- and high-cycle (i.e., thermal, mechanical) fatigue.

- Component and piping support structural integrity should be maintained with no reduction in margin for the final safety analysis report (FSAR) loading combination that governs their design.

- The LBB approach should not be considered applicable if there is a high probability of degradation or failure of the piping from more indirect causes such as fires, missiles, damage from equipment failures (e.g., cranes), and failures of systems or components in close proximity.

- The LBB approach should not be considered applicable to high-energy piping, or portions thereof, for which verification has not been provided that the requirements of I&E Bulletin 79-14 have been met.

- The LBB approach described in this report is limited in application to piping systems where the material is not susceptible to cleavage-type fracture over the full range of system operating temperatures where pipe rupture could have significant adverse consequences.

In addition, S.R.P. 3.6.3 (Reference 2) states that the piping system should be evaluated for the effects of creep damage, erosion, and environmental conditions. Furthermore, GDC 4 (Reference 3) requires that the piping system be evaluated for

indirect failure mechanisms and other degradation sources that could lead to pipe rupture. All of these requirements are addressed relative to the CF and LPI/DHR piping systems within the scope of this report in the following subsections.

2.1 Design Criteria

The containment was designed to accommodate a LOCA resulting from breaks in the reactor coolant pressure boundary up to and including a break equivalent in size to the double-ended rupture of the largest pipe in the reactor coolant system. It is not proposed to use the LBB results to modify these design criteria. Also, the functional design basis of the emergency core cooling system is unchanged from the original design basis and remains a nonmechanistic pipe rupture.

2.2 Susceptibility to Failure

This section addresses susceptibility of the systems to failure from the effects of corrosion, water/steam hammer, thermal and mechanical cyclic fatigue, erosion, creep, and cleavage type failure.

2.2.1 Corrosion

General corrosion is the uniform attack of a metal surface resulting in material dissolution and sometimes corrosion product buildup. Austenitic stainless steel is resistant to general corrosion.

Pitting and crevice corrosion are generally associated with stagnant or low flow conditions. Pitting corrosion can be considered a special instance of crevice corrosion in that when a pit is formed, it essentially becomes a crevice. Corrosion in crevices may be caused by (1) an increase in metal ion concentration within the crevice as compared with the concentration outside the crevice (concentration cell corrosion), (2) a decrease in oxygen concentration inside the crevice (oxygen concentration cell corrosion), or (3) increased corrodent activity resulting from the accumulation of corrosion products within the crevice (stagnant area corrosion). All three of these mechanisms are the result of restricted fluid circulation through the crevice. Restrictions on halogens and oxygen content have been found to contribute significantly to the control of the aforementioned mechanisms that cause pitting and crevice corrosion. It is unlikely that the conditions necessary for crevice or pitting corrosion of stainless steel piping exist even in stagnant or low flow areas of the Core Flood and LPI/DHR piping systems.

Stress corrosion cracking (SCC) is cracking of a metallurgically susceptible material under the combined action of stress and corrosion. Three factors (stress, corrosive environment, and material susceptibility) are necessary to initiate SCC.

- Tensile stress is required for SCC to occur. As the imposed tensile stress increases, the likelihood of initiation and accelerated propagation of SCC cracking increases. Generally, stresses close

to the material yield strength are required in a light water reactor environment to initiate SCC. Stress can be applied (as by operation), can be residual (as from fabrication), or can be a combination of applied and residual.

- SCC crack initiation also requires exposure to a corrosive environment particular to the material. For example, excessive levels of halogens, oxygen, and sulfates increase the susceptibility of austenitic stainless steels to SCC.

- For SCC to initiate, the material must be metallurgically susceptible. Chemical composition and metallographic condition affect the susceptibility of a metal to SCC. In some stainless steels and high nickel alloys, slow cooling through the 800-1500°F temperature range allows the precipitation of chromium carbides at grain boundaries, depleting the area adjacent to the grain boundaries of chromium. This process is termed "sensitization" and renders the material susceptible to SCC.

All stainless steel piping components within the scope of this report are forged products fabricated from wrought austenitic stainless steel. Austenitic stainless steels are corrosion resistant, iron-base alloys with high chromium and nickel contents. The austenitic stainless steel components were initially annealed to minimize susceptibility to sensitization. The stainless steel pipe weldments could become sensitized under some circumstances. Proper chemistry controls, as discussed below, are in place to protect the weldments and the heat-affected zones from cracking.

Reactor coolant chemistry controls are in place, as required by DPC Oconee Nuclear Station Selected Licensee Commitment, to prevent the coolant from becoming an environment favorable to SCC. Dissolved oxygen, halides, and other impurities in the primary coolant are monitored by plant surveillance testing in accordance with DPC Oconee Nuclear Station Selected Licensee Commitment 16.5.7.1 and are maintained in accordance with the EPRI PWR Primary Water Chemistry Guidelines for all modes of operation. Actual dissolved oxygen concentrations are usually maintained below 2 ppb by applying a hydrogen overpressure to the coolant system (25-50 cc/kg H_2O). During shutdown, the aerated primary coolant may contain as much as 8 ppm dissolved oxygen, but is below the temperature range where SCC is typically observed. Based on the above chemistry controls, it is concluded that an environment conducive to SCC of austenitic stainless steel piping does not exist in the Oconee Unit 3 CF and LPI/DHR piping systems.

In October of 2000, V.C. Summer plant experienced cracking in an Alloy 82/182 weld between the RV nozzle and the "A" loop hot leg piping. The cracking was primarily attributed to PWSCC. The bi-metallic weld between the core flood nozzle of the RV and the safe-end (at both the train "A" and train "B" locations) is fabricated from Alloy 82/182 weld metal. As a result of PWSCC issues associated with these bi-metallic welds, they

are excluded from this LBB evaluation. However, the Alloy 82/182 welds at both CF Tanks are included within the scope of this LBB evaluation. PWSCC is not considered an issue at these locations due to the low temperature (125°F) of the fluid in the tanks and adjacent piping.

2.2.2 Water/Steam Hammer

The piping systems within the scope of this report have been reviewed to determine the potential for water/steam hammer events to occur. As described in NUREG-0582 (Reference 4), water/steam hammer events may be caused by the following phenomena: flow into empty or voided lines; rapid valve opening, closing, or instability; water entrainment in steam lines; column separation; steam bubble collapse; slug impact due to rapid condensation; and pump startup, stopping, or seizure. System designs and operating experience as well as industry experience formed the basis of this evaluation. NUREG/CR-2781 (Reference 5) evaluated 40 reported water hammer incidents in pressurized water reactors. The evaluations for the systems in this program demonstrated that although the systems were susceptible to the generic causes of water/steam hammer, water hammer events were improbable and the severity of the reported incidents was low. Note that all reported water/steam hammer events resulted in only support damage. There were no events in the CF or LPI/DHR piping systems that resulted in a loss of pressure boundary integrity. Additional studies based on industry experience have reached the same conclusions and have provided recommendations for mitigating the causes of water/steam hammer in these systems (Reference 6).

Discussed below is the potential for water/steam hammer in the piping systems and the operating procedures used to minimize this potential.

- Core Flood System (CF)

  The core flood system is pressurized by a nitrogen cover. There are no pumps of any type in the line. The water is stagnant during normal operating conditions and is at low temperature. Therefore, the possibility of water/steam hammer in the core flood system is remote except during a postulated loss of coolant accident (LOCA).

- Low Pressure Injection/Decay Heat Removal System (LPI/DHR)

  NUREG/CR-2781 (Reference 5) identified a single water hammer event in a pressurized water reactor DHR system. The probable cause was reported as pump startup into a voided line during a refueling shutdown.

  The elimination of voids in the LPI/DHR system is achieved through required venting procedures during initial line fill and after component testing. During normal plant operation, portions of the

LPI/DHR system in containment are pressurized by the CF systems and are at building ambient or low temperature; therefore, a reduction in pressure will not result in the formation of a steam bubble. Valve opening and closing times, as well as pump startup or trip times, are determined to be of sufficient duration to produce negligible effects on the portion of the LPI/DHR system in the scope of this evaluation.

2.2.3 Thermal and/or Mechanical Cyclic Fatigue

For all piping within the scope of this LBB evaluation, normal and upset thermal and seismic loadings were evaluated as part of the piping stress analysis. The only unidentified operating condition in the CF and LPI/DHR systems that might contribute to fatigue is thermal stratification.

Thermal stratification usually occurs in horizontal pipe segments when fluid at a significantly different temperature than the fluid in the piping is introduced at low flow velocities. When the fluid's buoyancy forces are greater than the inertial forces acting on the fluid, the flow tends to separate into hot and cold layers. Thermal stratification has been identified in NRC Notice 84-87, "Piping Thermal Deflection Induced by Stratified Flow," and NRC Bulletins 79-13, "Cracking in Feedwater System Piping," 88-11, "Pressurizer Surge Line Thermal Stratification."

As required by NRC Bulletin No. 88-08, including Supplements 1 and 2, a review of piping systems connected to the RCS was performed to determine susceptibility to thermally stratified flow. The review determined that the piping systems within the scope of this evaluation were not susceptible to thermal stratification or temperature oscillations induced by leaking valves (Reference 7). Also, previous industry operating experience has not identified thermal stratification in these systems.

2.2.4 Erosion, Erosion/Corrosion, Erosion/Cavitation

There is no significant degradation from the effects of erosion and erosion/corrosion of the CF and LPI/DHR system piping greater than 8" in diameter (Reference 8). There is no degradation due to erosion/cavitation because there are no pumps or throttling valves in these lines. Control of water chemistry as discussed above provides additional protection from erosion/corrosion for the systems connected to the RCS.

2.2.5 Creep

Creep and creep-fatigue is not a concern as all operating temperatures are well below the temperature of 800°F, at which creep and creep fatigue become a concern for austenitic stainless steel.

2.3 Component and Piping Supports

All equipment, piping and supports within the scope of this evaluation have been seismically designed per the rules of USAS B31.7 and USAS B31.1. The removal of the dynamic effects due to pipe rupture from the design basis of the supports does not reduce the margin of safety of any supports.

2.4 Degradation or Failure from Indirect Causes

Application of LBB on the pipe lines in this scope would not increase the probability of degradation or failure of the piping from indirect causes. Effects on piping systems and components from indirect causes such as fires, missiles, and damage from equipment failures, and failures of systems or components in close proximity were evaluated and dispositioned during the original design of the Oconee stations (Reference 9) and during the design of the modification to this system.

All piping, components, and supports inside containment are designed seismically to prevent failures of safety-related piping and components as a result of failures of non-safety-related items. There are no snubbers attached to the piping within the scope of this evaluation.

2.5 I&E Bulletin 79-14 Verification

Safety-related piping systems at Oconee have been verified to the requirements of I&E Bulletin 79-14. Subsequent to 79-14 verification, modifications to safety-related piping systems are reviewed to verify that dimensional information is applicable.

2.6 Cleavage-Type Fracture Susceptibility

The piping systems within the scope of this evaluation are exposed to the normal system operating temperatures ranging from 125°F to 557°F for the CF and LPI/DHR systems. Cleavage-type fracture is not a concern for the piping material at these operating temperatures.

3. MATERIALS AND MATERIAL PROPERTIES

3.1 Tensile Properties of CFL Pipe Materials (Base Metal)

The piping systems within the scope of this report are made of ASTM A 376, Grades TP304H and TP316H, ASTM A 358, Class 1, Grade TP304, ASME SA-376, Grade TP316 and ASME SA-336 Class F8M as summarized in Table 3-1. They are made from a wrought product form. These piping systems do not contain any cast pipe or cast fittings. New check valves are installed as part of the cross tie modification. They are made of forged SA-182 F316 material. The remaining check valves in the CF line are made of A-351 CF8M cast product material which is addressed in Section 4.2.2. The tensile properties of the base metal materials of these piping systems are discussed below. They were obtained through review of the Certified Material Test Reports (CMTRs).

The piping (14" Schedule 30), adjacent to the core flood tanks is made of ASTM A 358, Class 1, Grade TP304 material. The room temperature material properties from these CMTRs are summarized in Table 3-2. Since this portion of the piping operates at only 125°F, the room temperature properties were considered appropriate. The yield strength for these piping materials range from 39,200 psi to 43,600 psi and the ultimate tensile strength range from 85,300 psi to 87,808 psi.

The piping (14" Schedule 140) adjacent to the reactor vessel is made of ASTM A 376, Grade TP316H material. The room temperature material properties from these CMTRs are summarized in Table 3-3. The yield strength for these piping materials is 42,400 psi and the ultimate tensile strength is 88,400 psi. Representative material properties at 550°F (near steady state operating temperature for this piping) were then determined for this material using ASME Code Section III (Reference 10). Ratios of the ASME Code tensile properties (property at 550°F divided by property at 70°F) were applied to the tensile properties given in Table 3-3 to obtain the plant specific properties for ASTM A 376, Grade TP316H material at 550°F as given in Table 3-4.

3.2 Weld Materials and Processes

The weld filler metals of the core flood piping systems are E308L, ER308, E308L-16, E316, E316L and E316-16. The weld processes that were used were Gas Tungsten Arc Weld (GTAW - also referred to as TIG weld) and Shielded Metal Arc Weld (SMAW). The piping between the core flood tank and the gate valve (line 14030-1 in Table 3-1) has longitudinal seam welds as well as circumferential seam welds. The circumferential seam weld between the safe-end at the core flood tank and the pipe is made using the GTAW weld process.

3.3 Material Properties for LBB Analysis

The tensile and fracture toughness properties used for the LBB analysis of the CF and LPI/DHR piping systems were primarily obtained from the experimental work of Landes and McCabe on austenitic stainless steel base metals and weldments (Reference 11). The tensile test properties of the base metal specimens compared very well with the base metal materials used for the actual piping. The tensile test properties of the piping material at the critical locations identified for LBB analysis were obtained from the CMTRs. From Section 4.2.3, the critical locations for LBB analysis were identified as (a) the piping adjacent to the core flood tank, and (b) the piping adjacent to the reactor vessel.

The piping adjacent to the core flood tank is made of Type 304SS material. The weld metal material process used for this portion of the piping is GTAW. The base metal material used for the piping adjacent to the reactor vessel is Type 316SS and the weld metal material process used is SMAW.

Determination of specific material properties such as the Ramberg-Osgood parameters and the material parameters for the J-R equation are given in Sections 3.3.2 and 3.3.3 respectively. The summary of the material properties used for the LBB analysis is provided in Section 3.3.4.

3.3.1 Tensile Properties - Specimen versus Actual Piping Materials

The tensile test results for the Type 304SS and Type 316SS base metal materials of the CF and LPI/DHR piping systems, as given in Tables 3-2 and 3-4, are comparable to the experimental results (Reference 11) for the respective materials as given in Tables 3-5 and 3-6.

For the piping adjacent to the core flood tank, made of Type 304SS, the yield strengths ranged from 39,200 psi to 43,600 psi and the ultimate tensile strength ranged from 85,300 psi to 87,808 psi. The yield and the ultimate strengths for the Type 304SS specimen tested were 40,900 psi and 85,800 psi, respectively.

At the operating temperature of 550°F, the yield and ultimate strengths of the Type 316SS piping adjacent to the RV are 27,300 psi and 84,600 psi, respectively. For the Type 316SS specimen, the yield and ultimate strengths were 33,200 psi and 72,700 psi, respectively. Since the yield strength for the actual piping material is lower than the Type 316SS specimen, the experimental data (stress-strain as well as J-R data) of the Type 304SS specimen, which had a lower yield strength, was used to ensure lower bound properties were used in the flaw stability analysis. The yield and ultimate strengths for the Type 304SS specimen were 23,700 psi and 61,900 psi, respectively.

3.3.2 Ramberg-Osgood Parameters

The Ramberg-Osgood stress-strain parameters (α and n) are determined in this analysis using the applicable experimental data (true stress-true strain) of the specimens (Reference 11). The following Ramberg-Osgood equation is fitted to the true stress-true strain data:

$$\frac{\varepsilon}{\varepsilon_0} = \frac{\sigma}{\sigma_0} + \alpha\left(\frac{\sigma}{\sigma_0}\right)^n \qquad (3\text{-}1)$$

where σ, ε - true stress, true strain
σ_0, ε_0 - yield stress, yield strain
α, n - Ramberg-Osgood material parameters

These parameters are determined by performing a Ramberg-Osgood stress-strain equation fit to the experimental data in the low strain range ($0.00 < \varepsilon < 0.15$ inches) as illustrated in Figure 3-1. This figure shows the true stress - true strain data and the corresponding Ramberg-Osgood equation fit to the Type 304SS data at 75°F. The curve fit in the low strain region provides the best results as indicated in Appendix A of NUREG 1061, Volume 3 (Reference 1). Since the true-stress true-strain data for Type 316SS at 550°F are not provided in Reference 11, the Ramberg-Osgood coefficients as derived for pipe ID#DP2-A50, Experiment ID# 4111-5, (Reference 12) which has similar yield and tensile strength data as the specimen data of Reference 11, are used.

3.3.3 Material Parameters for J-R Equation

The material parameters for the J-R equation (C and N) are determined in this analysis using the J deformation and Δa experimental data of the applicable compact tension specimens (Reference 11). The power law formula for the J-R data is obtained using a linear regression analysis and is given below:

$$J_D = C\Delta a^N \qquad (3\text{-}2)$$

where J_D is $J_{Deformation}$ in units of in-lbs/in^2, and C and N are the material parameters for a given specimen.

The resulting power law J-R curves for the base and weld metal (Type 304SS and GTAW at 75°F) of the piping at the core flood tank are depicted by Figures 3-2 and 3-3, respectively. For the Type 316SS base metal material of the core flood line at the reactor vessel, the J-R curves of Type 316SS and Type 304SS materials (at operating temperature of 550°F) are used as provided in Figures 3-4 and 3-5. The J-R curve for the Type 304SS material ensures use of lower bound base metal material properties for this portion of the piping. The J-R curve for the SMAW weld metal material at 550°F is given in Figure 3-6. These figures show a very good power law fit to the J-R data.

3.3.4 Summary of LBB Material Properties

Table 3-5 provides a summary of the material properties used in the LBB analysis of the low pressure piping that is attached to the core flood tank. This region of the piping system, which lies between the core flood tank and the electric motor operated (EMO) gate valve (3CF-1 or 3CF-2), is 14" schedule 30 piping with a normal operating temperature of 125°F. The material properties that are available, particularly for the J-R curve, are for either 75°F (room temperature) or for 550°F. For this application, the material properties at 75°F are considered appropriate.

Table 3-6 provides a summary of the material properties for the LBB analysis of the 14" schedule 140 high pressure portion of the CFL piping. This region of the piping system operates at a steady state temperature of 557°F. The material properties, derived at 550°F, are considered appropriate for this application.

Table 3-1 Base Metal Materials for CF and LPI/DHR System Piping

Piping System	Line No.[1]	Description	Material Specification
CF	14030-1	CF Tank to Gate Valve (3CF-1, 3CF-2)	ASTM A 358, Cl. 1, Gr. TP304
CF	---	Safe-End to CF Tank Outlet Nozzle	ASME SA-376, Gr. TP316
CF	14140-2	Gate Valve (3CF-1, 3CF-2) to 2nd 14" Check Valve (3CF-12, 3CF-14)	ASTM A 376, Gr. TP304H
CF	14140-3	Second 14" Check Valve (3CF-12, 3CF-14) to RV	ASTM A 376, Gr. TP316H
CF	----	Safe-End to CF Nozzle at RV	ASME SA-336, Cl. F8M
LPI/DHR	10140-5	New 10" Check Valve (3LP-176, 3LP-177) to CF Line	ASTM A 376, Gr. TP304H

[1] The piping system line numbers are as defined in Section 1. Note that the unit and train identifiers (e.g. 3A) are not included as the line numbers, descriptions and material specifications are the same for each train.

Table 3-2 Room Temperature Tensile Properties for Piping Adjacent to Core Flood Tanks (Base Metal)

Heat No.	Yield Strength, psi	Ultimate strength, psi
2P4640	43,600	85,300
2P4640	39,200	87,808

Table 3-3 Room Temperature Tensile Properties for Piping Adjacent to Reactor Vessel (Base Metal)

Heat No.	Yield Strength, psi	Ultimate strength, psi
F0657	42,400	88,400

Table 3-4 Tensile Properties at 550°F (ASME Code adjusted)[1] for Piping Adjacent to Reactor Vessel (Base Metal)

Yield Strength, psi	Ultimate strength, psi
27,300	84,600

[1] The ASME Code adjusted values are obtained by a ratio procedure as explained in Section 3.1.

Table 3-5 Material Properties for LBB Analysis of Piping Adjacent to Core Flood Tank at 75°F

Material Property	Type 304SS Base Metal	GTAW Weld Metal
yield strength, σ_y, ksi	40.9	68.9
ultimate strength, σ_{ult}, ksi	85.8	90.5
reference strain, ε_o, in/in	0.00145	0.0024
Young's Modulus, E, ksi	28060	28060
Ramberg-Osgood stress-strain parameters:		
α	13.6	6.25
n	4.0	6.8
Material parameters in J-R eqn.		
C	57100	55400
n	0.8	0.8

Table 3-6 Material Properties for LBB Analysis of Piping Adjacent to Reactor Vessel at 550°F

Material Property	Type 316SS Base Metal	Type 304SS Base Metal	SMAW Weld Metal
yield strength, σ_y, ksi	33.2	23.7	49.4
ultimate strength, σ_{ult}, ksi	72.7	61.9	64.7
reference strain, ε_o, in/in	0.00093	0.00093	0.0019
Young's Modulus, E, ksi	25500	25500	25500
Ramberg-Osgood stress-strain parameters:			
α	0.565	8.0	16.5
n	8.28	3.5	7.25
Material parameters in J-R eqn.			
C	28200	17700	5100
n	0.63	0.5	0.38

Figure 3-1 True Stress - True Strain for Type 304SS at 75°F

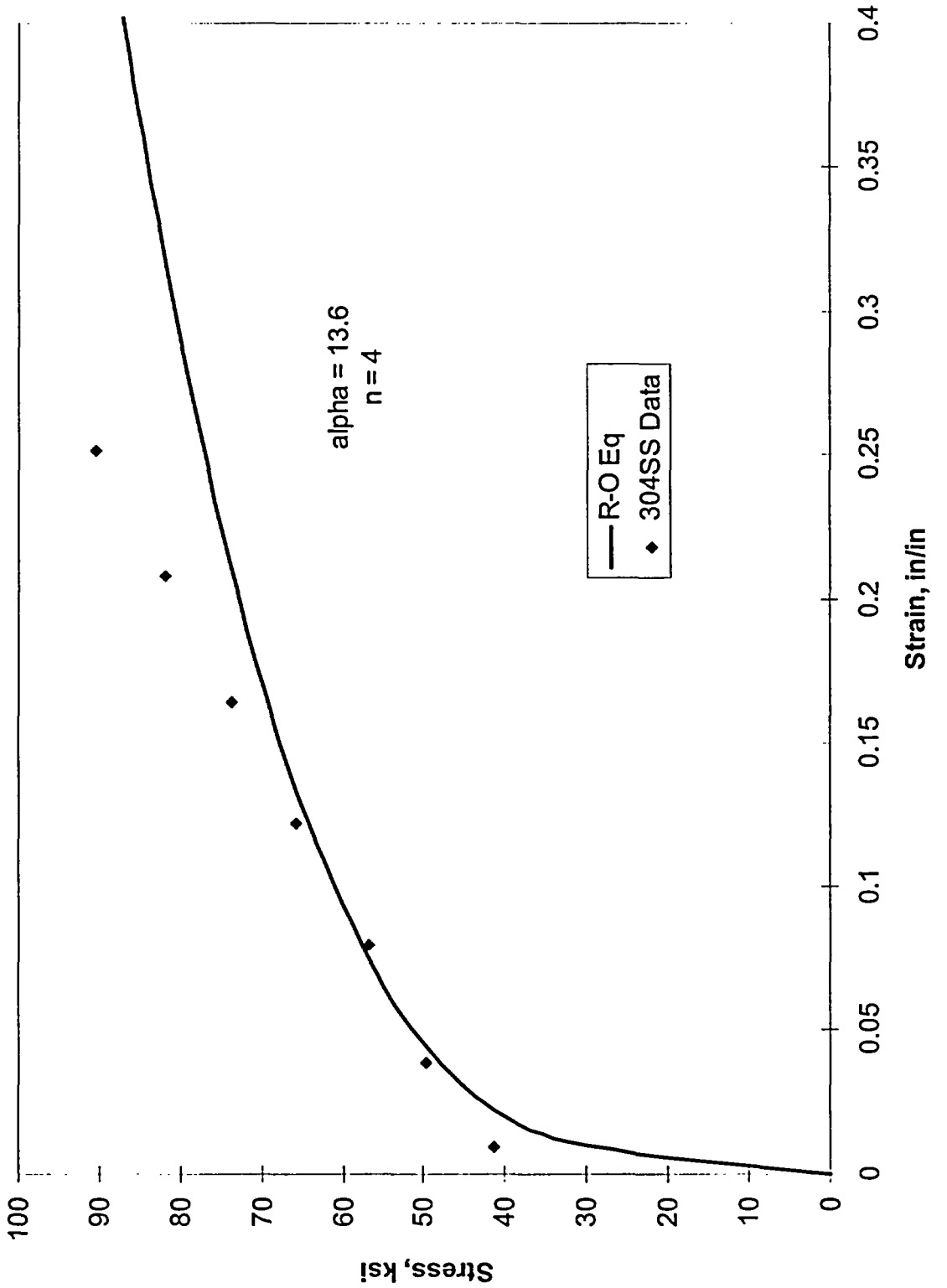

AREVA

Figure 3-2 J-R Curve for Type 304SS at 75°F

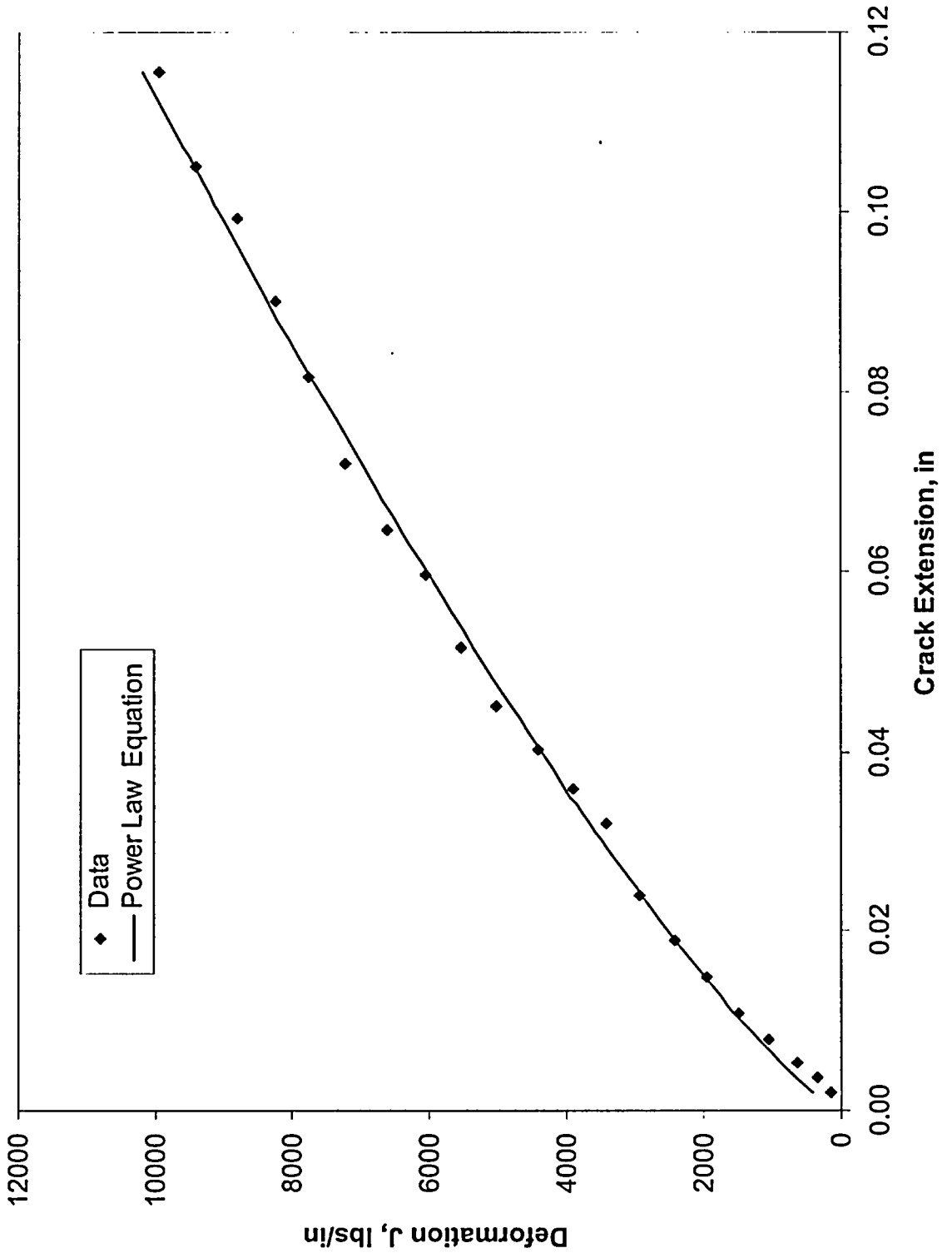

AREVA

Figure 3-3 J-R Curve for GTAW Weld Metal at 75°F

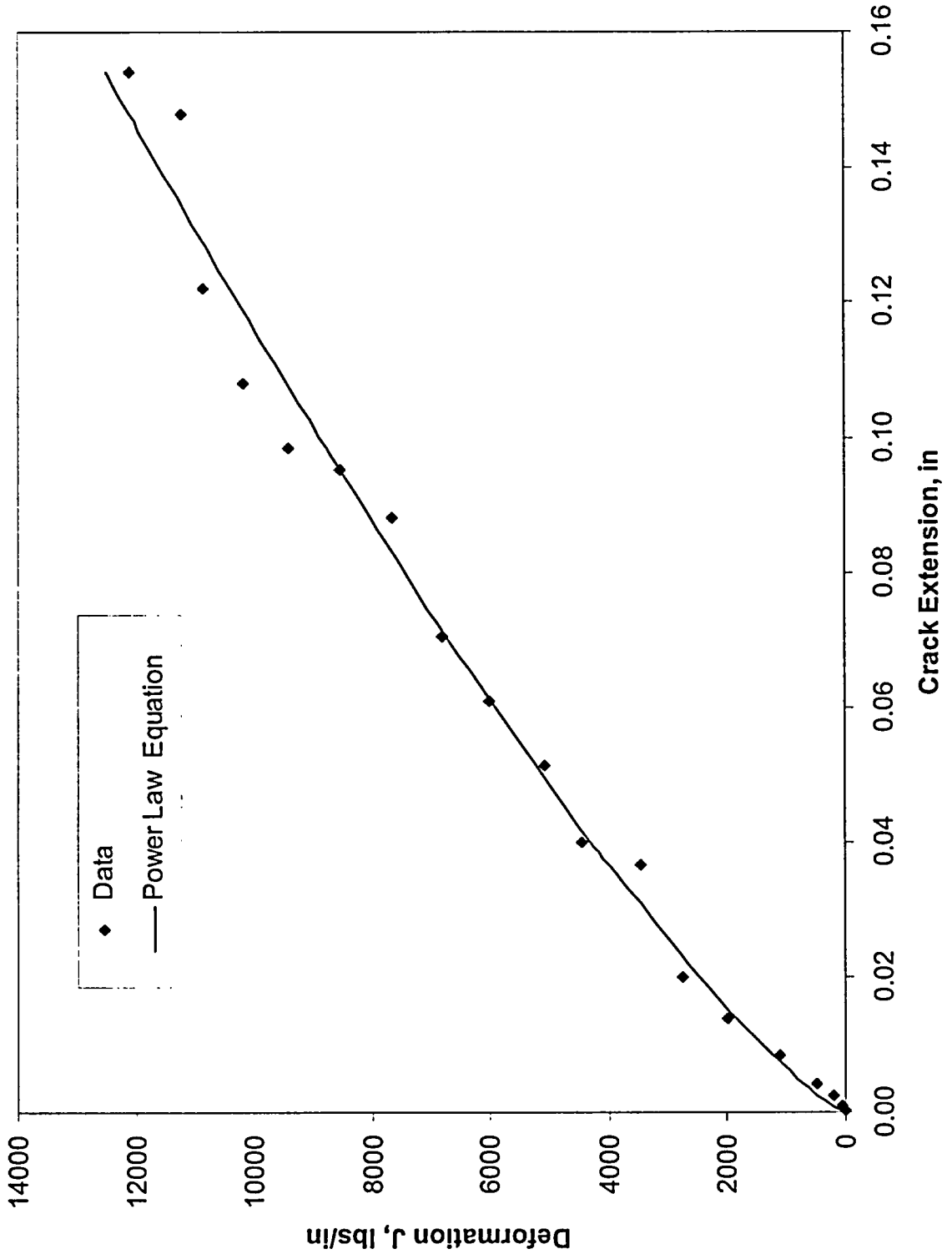

AREVA

Figure 3-4 J-R Curve for Type 316SS Base Metal at 550°F

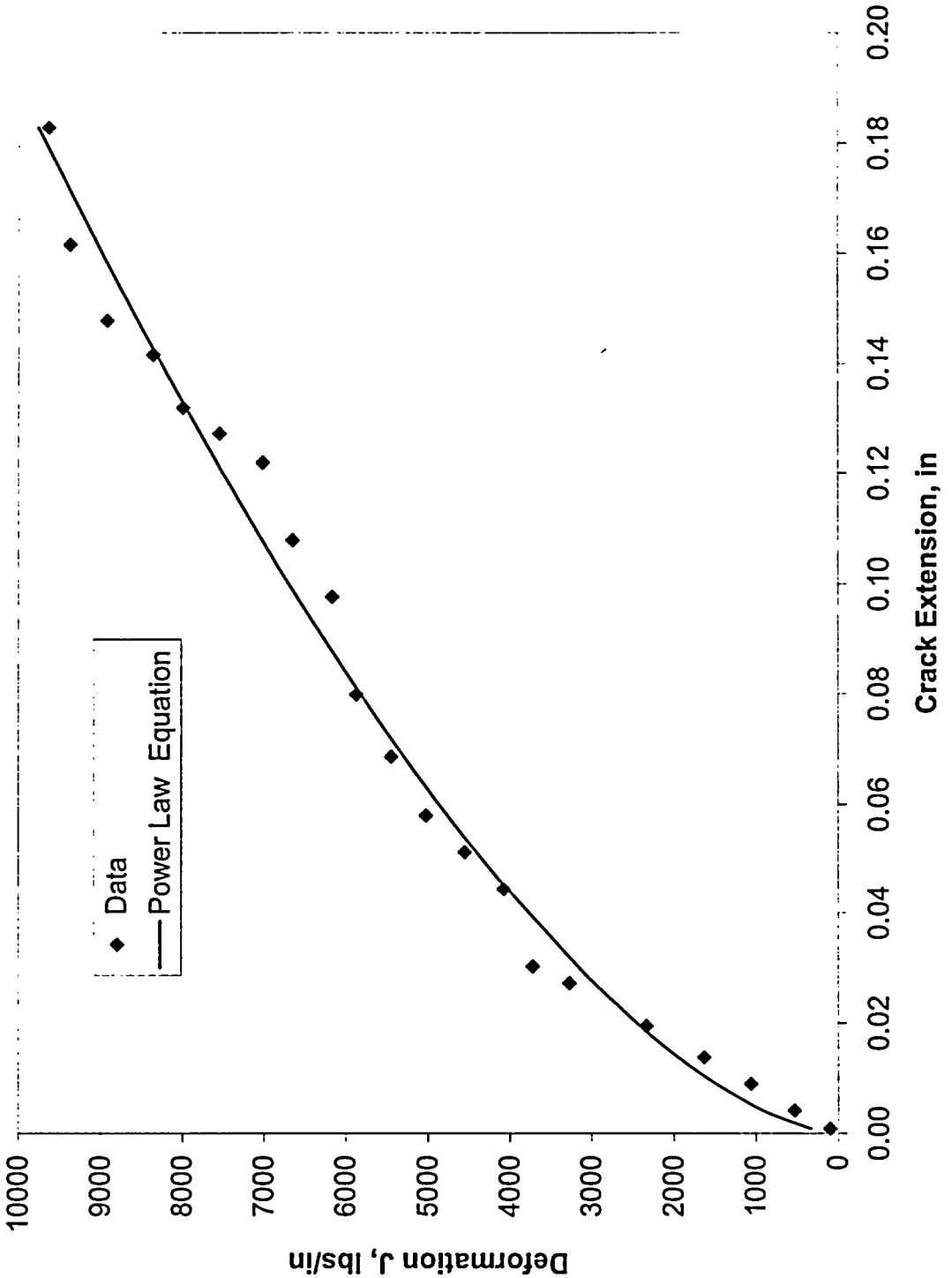

AREVA

Figure 3-5 J-R Curve for Type 304SS Base Metal at 550°F

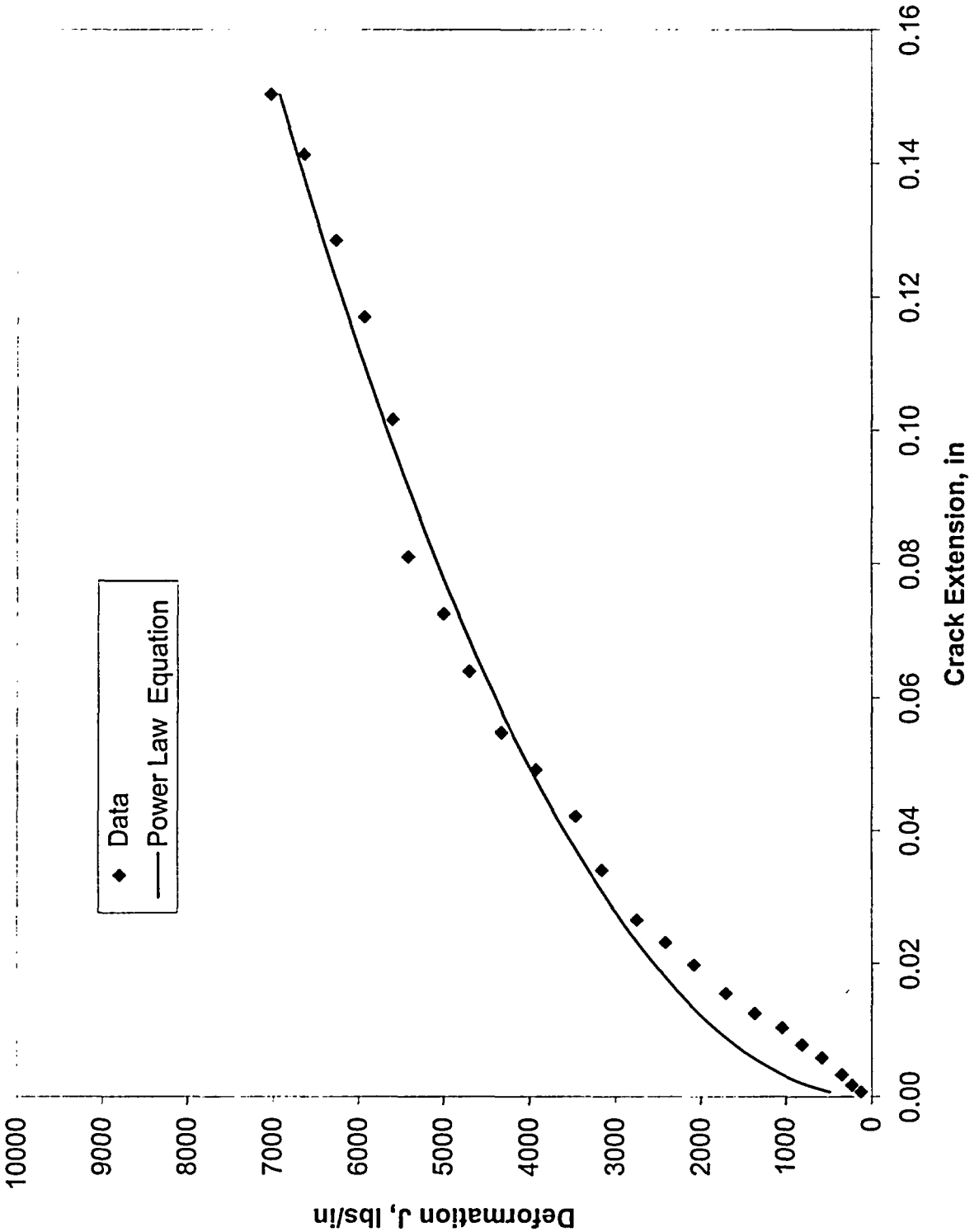

AREVA

Figure 3-6 J-R Curve for SMAW Weld Metal at 550°F

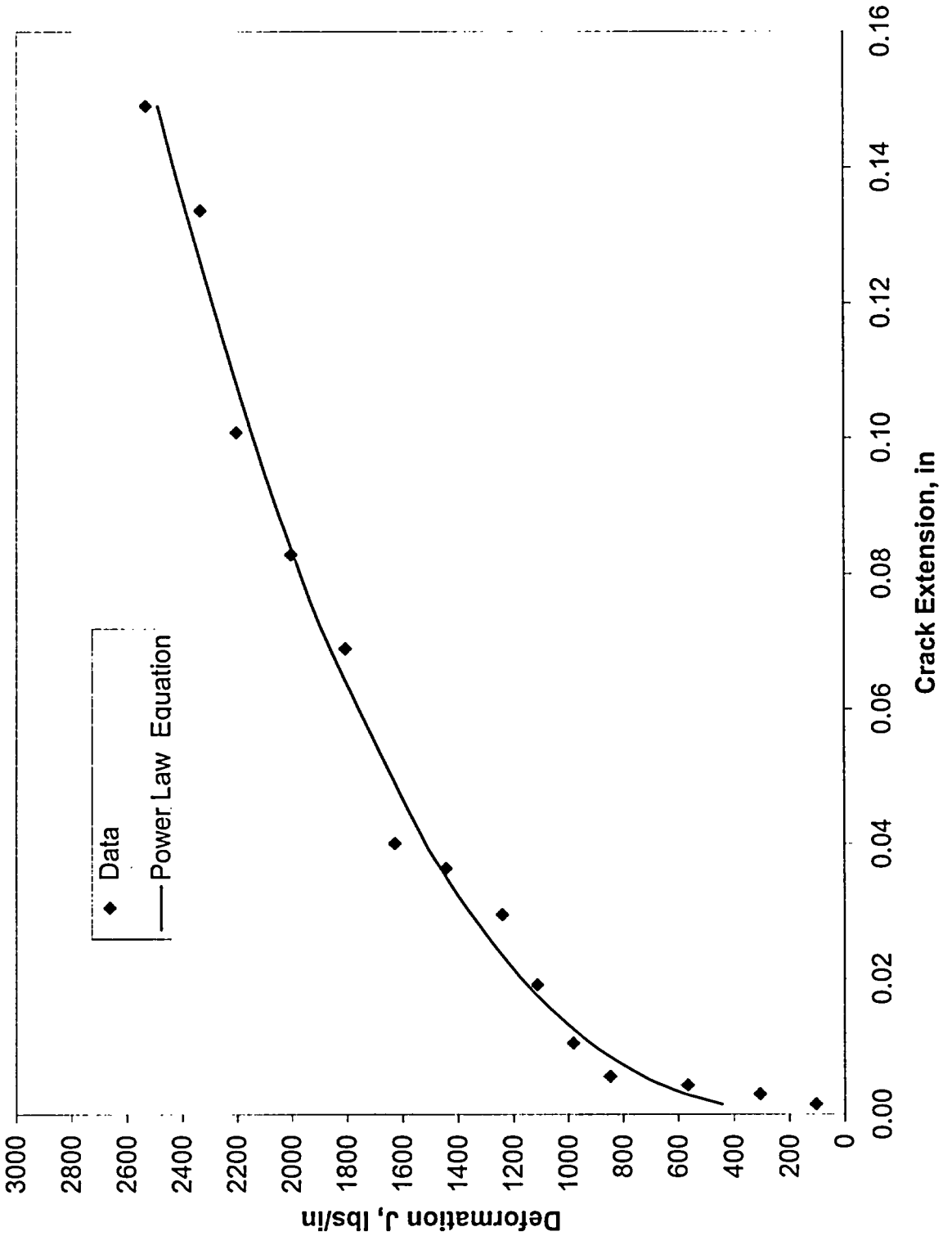

AREVA

4. APPLIED LOADINGS AND SELECTION OF LOCATIONS FOR LBB

4.1 Applied Loadings

The applied loadings on the CF and LPI/DHR piping systems of Oconee Unit 3 are determined from the current piping stress analysis for the installed piping and support configuration with the new LPI cross tie modification. The applied loadings considered for LBB analysis consist of minimum moment loadings for leakage crack size evaluation and maximum moment loadings for flaw stability evaluation as described in Sections 4.1.1 and 4.1.2.

4.1.1 Minimum Moments

The minimum moment loads for the LBB evaluation are based on normal operating conditions. These loads are used for the determination of the 10 gpm leakage flaw sizes. The moment loadings considered are deadweight and thermal expansion loads corresponding to 100% power steady state conditions. The minimum moment is obtained by algebraically summing the individual components of moments due to deadweight and thermal expansion and then computing its square-root sum of the squares (SRSS) value to yield the resultant moment (Mr). The minimum moment and the operating pressure are normally present during steady state conditions and tend to open an existing crack to allow leakage flow.

4.1.2 Maximum Moments

The maximum moment loads considered in the flaw stability calculations of the LBB analysis are calculated by combining the minimum moment loads with the moments due to safe shutdown earthquake (SSE) and SSE seismic anchor motions (SSE SAM). The maximum moment can be determined using the algebraic load combination method or the absolute sum load combination method per S.R.P. 3.6.3. For this analysis, the absolute sum load combination method is selected. The formulas for the absolute sum load combination method are given in S.R.P. 3.6.3 and shown below.

Axial Force:

$$F_{combined} = |F_{Deadweight}| + |F_{Thermal}| + |F_{Pressure}| + |F_{SSE}| + |F_{SAM}| \quad (4\text{-}1)$$

Components of Moment:

$$(M_i)_{Combined} = |(M_i)_{Deadweight}| + |(M_i)_{Thermal}| + |(M_i)_{Pressure}| + |(M_i)_{SSE}| + |(M_i)_{SAM}| \quad (4\text{-}2)$$

where i = 1, 2, 3

Resultant Moment:

$$M_{Resultant} = [(M_1)^2_{Combined} + (M_2)^2_{Combined} + (M_3)^2_{Combined}]^{0.5} \quad (4\text{-}3)$$

The individual components of bending moment (M_1, M_2, M_3) due to deadweight, thermal expansion, safe shutdown earthquake (SSE), and SSE seismic anchor motions are calculated by summing the loads absolutely (without consideration of signs). The resultant moment (Mr) is then determined by calculating the SRSS value of the individual components of the moments. The axial force is determined by summing the absolute values of the axial forces due to deadweight, thermal expansion, pressure, SSE, and SSE SAM.

4.2 Selection of Locations for LBB Analysis

The maximum moment loadings of the CF and the small portion of the high energy LPI/DHR piping are reviewed to identify the highest stress locations for LBB analysis. For a given pipe size, the locations that are candidates for LBB analysis are those that have the least favorable combination of stress and material properties per S.R.P. 3.6.3. Identification of the highest stressed location and subsequent consideration of the local material properties (base metal, weldments and, if applicable, safe-ends), including the worst case material properties, helps ensure the proper selection of locations for LBB analysis. Identification of the most highly stressed location is discussed in Section 4.2.1 and the consideration of fracture toughness is discussed in Section 4.2.2. Finally, the selection of locations for LBB analysis is provided in Section 4.2.3.

4.2.1 Consideration of High Stress Locations

The highest stressed locations are identified first. The CF piping system contains 14" schedule 140 piping (high pressure and low pressure portions) from the reactor vessel to gate valve 3CF-1 (train "A") or 3CF-2 (train "B") and contains 14" schedule 30 piping (low pressure portion) from the gate valve to the core flood tank. The LPI/DHR piping contains 10" schedule 140 piping (low pressure line). Based on the review of the maximum moment loadings, the most highly stressed location in the high pressure and high temperature piping systems within the scope of this report is the core flood piping adjacent to the reactor vessel. This location is expected to be highly stressed as it is attached to the reactor vessel and is in the high pressure region of the piping system. Since a portion of the CF line is made of a thinner wall piping (schedule 30 piping), the most highly stressed location within this part of the piping is also identified for LBB evaluation. In this region, the core flood piping adjacent to the core flood tank is identified as the most highly stressed (Reference 13).

4.2.2 Consideration of Fracture Toughness

The CF and LPI/DHR piping system contains Type 304 or Type 316 stainless steel and is circumferential seam welded using the SMAW welding process. The only region where a different welding process is used is the piping between the core flood tank and the gate valve. This piping uses a GTAW welding process which has better material toughness properties than the SMAW welding process.

The base metal material used for the piping adjacent to the reactor vessel (most highly stressed region in the entire CF and LPI/DHR piping system) is Type 316 stainless steel. Since the material properties for Types 304SS and 316SS are similar, and Type 304SS provides lower bounding fracture toughness properties (refer to Section 3), the properties of both materials are considered in the evaluation of this location. The circumferential seam welds in this portion of the piping use the SMAW welding process. Therefore, its properties are considered in the analysis of this location. Since this part of the piping operates at or near 550°F, the material properties at this temperature were considered in the evaluation.

The piping adjacent to the core flood tank contains Type 304SS (base metal) and uses a GTAW welding process (weld metal). This portion of the piping operates at low temperature (125°F). Therefore, material properties (for base and weld metals) at room temperature are considered appropriate and used in the analysis of this location.

The 14 inch check valves in the CF system piping are the only components that are made of cast stainless steel (A-351 CF8M). Cast stainless steel materials are susceptible to a loss of fracture toughness through thermal embrittlement at operating temperatures of 525°F and above (Reference 14). The only check valve that operates at elevated temperatures is the 14 inch check valve (3CF-12 and 3CF-14) closest to the RV. The operating temperature of this check valve is conservatively calculated as 330°F (Reference 13). Furthermore, the applied bending stresses due to minimum and maximum moment are 40 percent and 56 percent, respectively, of the stresses in the piping adjacent to the reactor vessel. Therefore, this check valve is bounded by the piping adjacent to the reactor vessel which is already identified for LBB analysis.

4.2.3 Selection of Locations

Based on consideration of the high stress locations coincident with worst case material properties, the critical locations for LBB analysis are identified as:

Location 1: Core Flood Piping Attached to Bottom of the Core Flood Tank Nozzle
Location 2: Reactor Vessel Core Flood Nozzle Safe-End to Pipe Juncture

The selected locations for LBB analysis are depicted in Figure 4-1. The applied loadings at these two locations are provided in Tables 4-1 and 4-2.

Table 4-1 Applied Loads at Critical Location 1

Temperature = 120°F
Pressure = 600 psig
Outside Diameter = 14 in
Thickness = 0.375 in
Material = Type 304 Stainless Steel

Loading Condition	Faxial (kips)	Ma (in-kips)	Mb (in-kips)	Mc (in-kips)	Mr (in-kips)
Weight	1.7	41.8	-19.0	-11.5	
Pressure	82.7				
Thermal	0.9	-60.6	-72.1	30.0	
SSE	6.9	200.0	708.8	378.0	
SSE SAM	0.2	3.1	15.3	6.4	
Normal Operating (Min. Moment)	85.3	-18.8	-91.1	18.5	94.8
Faulted (Max. Moment)	92.4	305.5	815.2	425.9	969.2

Table 4-2 Applied Loads at Critical Location 2

Temperature = 554°F
Pressure = 2185 psig
Outside Diameter = 14 in
Thickness = 1.25 in
Material = Type 316 Stainless Steel

Loading Condition	Faxial (kips)	Ma (in-kips)	Mb (in-kips)	Mc (in-kips)	Mr (in-kips)
Weight	0.5	32.4	-46.1	-291.6	
Pressure	227.0				
Thermal	0.1	-34.3	3.3	-82.8	
SSE	7.8	602.5	486.1	469.7	
SSE SAM	0.2	19.9	24.3	10.3	
Normal Operating (Min. Moment)	227.6	-1.9	-42.8	374.4	376.8
Faulted (Max. Moment)	235.6	689.1	559.8	854.4	1232.2

Figure 4-1 Isometric View of CF/LPI/DHR Piping System Critical Locations

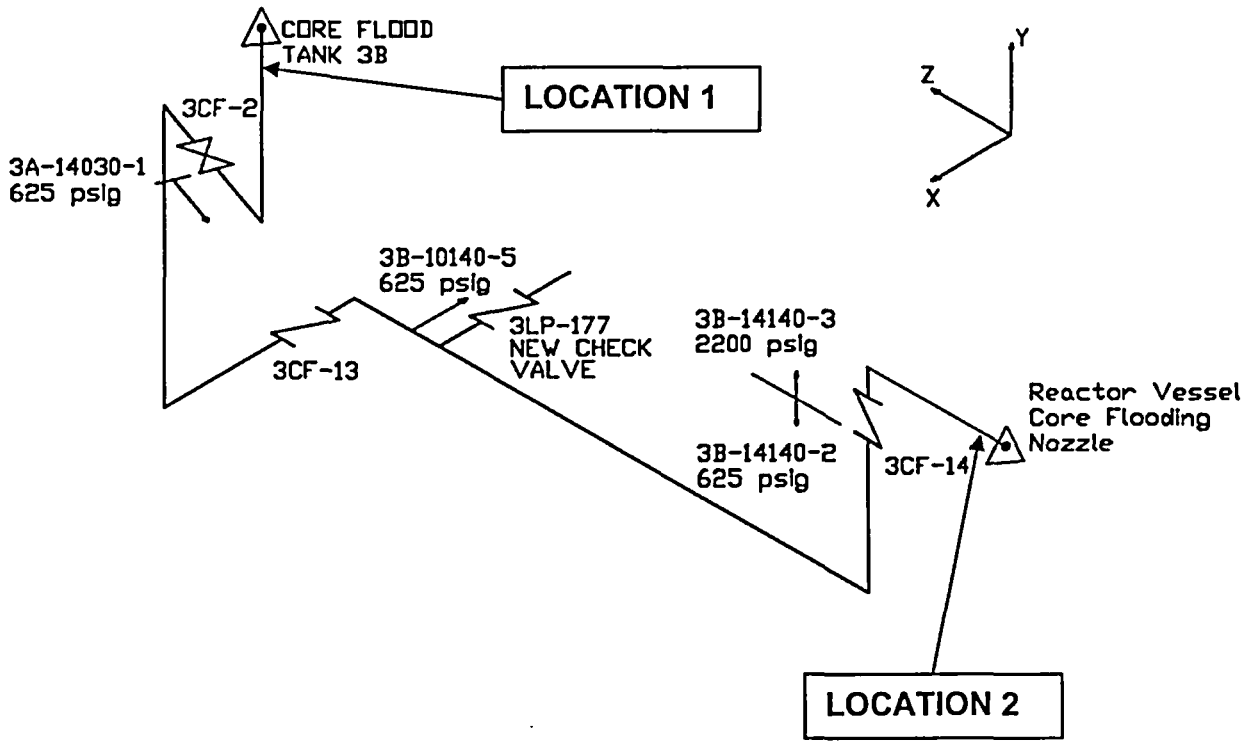

AREVA

5. LEAK DETECTION

General Recommended Action 3 in the Executive Summary of NUREG-1061, Volume 3 (Reference 1) states that:

> Leak detection systems in existing nuclear plants should be examined on a case-by-case basis to ensure that suitable detection margins exist so that the margin of detection for the largest postulated leakage size crack used in the fracture mechanics analyses is greater than a factor of ten on unidentified leakage. Licensees and applicants have the option of requesting a decrease in leakage margin provided they can confirm that their leakage detection systems are sufficiently reliable, redundant, diverse, and sensitive.

This section addresses the Oconee leakage detection system for the purpose of demonstrating the acceptability of utilizing 1 gpm as the minimum detectable leak.

5.1 Limiting Condition for Operation

Technical Specification 3.4.13 addresses the reactor coolant system (RCS) leakage detection system. The Oconee limiting condition for operation for RCS leakage is specified as 1 gpm unidentified leakage. Unidentified leakage is defined as all leakage that is not:

- seal water flow supplied to the reactor coolant pump seals (controlled leakage);
- leakage into the containment atmosphere from sources that are both specifically located and known either not to interfere with the operation of leakage detection systems or not to be leakage through a non-isolable fault in an RCS component body, pipe wall or vessel wall; or
- RCS leakage through a steam generator to the secondary coolant system.

This LBB analysis is based on the minimum detectable through wall leakage for the applicable piping systems. The RCS pressure boundary leak detection system is consistent with the guidelines of Regulatory Guide 1.45 (Reference 15) such that leakage of 1 gpm in one hour can be detected. Therefore, the LBB analysis uses the 1 gpm limiting condition for operation as an upper limit for RCS leakage.

5.2. Major Leak Detection System Components

The reactor coolant leakage detection system is discussed in Section 5.2.3.10.3 of the Oconee Updated Final Safety Analysis Report (UFSAR). Technical Specification 3.4.15 requires that at least two reactor coolant leakage detection systems be operational with one of the two systems being sensitive to radioactivity. Leakage can be continuously monitored in the control room by surveillance of the following detection systems:

- the reactor building atmosphere particulate radioactivity monitoring system,
- the reactor building normal sump level indicators,
- the reactor building iodine, gaseous radioactivity and area monitoring systems,
- the reactor coolant constant inventory measurement system.

6. LEAKAGE SIZE CRACK DETERMINATION

Leakage size crack (LSC) determination for the Oconee CF and LPI/DHR piping within the scope of this analysis is performed in accordance with Proposed SRP 3.6.3 (Reference 2). The LSC determination is performed as a two step process as described below.

6.1 Crack Opening Area Analysis

In the LBB analysis within the scope of this report, two types of flaws are considered: circumferential and longitudinal. Circumferential flaws are sensitive to internal pressure and externally applied axial loads and moments. Longitudinal flaws are sensitive to internal pressure.

In the circumferential crack opening area analysis, the normal operating loads (deadweight + normal operating thermal + pressure) tabulated in Section 4 are used to calculate the crack opening displacement (COD) for a range of hypothetical crack lengths. The determination of the COD for a circumferential through-wall crack is based on the GE/EPRI elastic-plastic method (Reference 16). The crack opening area is then calculated from the COD and the hypothetical crack length by assuming an elliptical shape.

In the longitudinal crack opening area analysis, the only applicable normal operating load is pressure. The determination of the crack opening area for a longitudinal through-wall crack is based on the Paris-Tada linear elastic fracture mechanics correlation (Reference 17).

The only material property used for the crack opening area analyses is the Young's Modulus. The Young's Moduli used in the analyses are shown in Table 6-2 and are taken from the code of record (Reference 18). The GE/EPRI method requires Ramberg-Osgood parameters and yield strength values when considering plasticity in the crack opening area calculation. Consideration of plasticity is not required in these analyses due to the low stress levels found in the critical locations during operating conditions.

6.2 Leak Rate Analysis

The crack opening area discussed above is used in the FANP program KRAKFLO (Reference 19) to determine the crack length necessary to obtain the required 10 gpm leak rate. KRAKFLO calculates single phase and two phase flow through a slit considering parameters such as system pressure, temperature, flaw surface roughness, pipe dimensions, and flow area resulting from applied loads. The leak flow calculation used in KRAKFLO is benchmarked against the Battelle Columbus Laboratories data as

presented in Reference 20. KRAKFLO is based on the LEAK-01 program documented in Reference 20, but has improved ability to determine pressure drops for initially subcooled non-flashing liquid.

6.3 Results

As discussed above, the leakage size crack (LSC) is defined as the crack size allowing a 10 gpm leak rate. Table 6-1 presents the LSC length for the circumferential and longitudinal cracks evaluated in this report (Reference 13).

Table 6-1 Leakage Size Cracks

Critical Location	Crack Type	Leakage Size Crack Length (in)
1	Circumferential	6.42
2	Circumferential	6.87
1	Longitudinal	4.39
2	Longitudinal	5.11

Table 6-2 Crack Opening Area Analysis Material Properties

Critical Location	Material	Temperature	Young's Modulus ($\times 10^{-6}$ psi)
1	Type 304 SS	120°F	28.07
2	Type 316 SS	554°F	25.72

7. FLAW STABILITY ANALYSIS

7.1 General Methodology

7.1.1 Acceptance Standards for LBB Analysis

S.R.P. 3.6.3 (Reference 2) provides the acceptance standards for the leak-before-break analysis for commercial nuclear reactor piping. S.R.P. 3.6.3 indicates that two types of analyses must be performed: one for determining the margin on flaw size, and another for determining the margin on load. When the algebraic sum load combination method is utilized, S.R.P. 3.6.3 requires a margin of two on flaw size and a margin of 1.4 on the applied loading. However, when the absolute sum load combination method is used, the margin on the applied loading is reduced to 1.0.

The absolute sum load combination method is used in the analysis. Therefore, a factor of two on the flaw size is the only requirement that must be addressed. S.R.P. 3.6.3, review procedure item 10e requires a fracture mechanics flaw stability analysis or a limit load analysis. A flaw stability analysis is performed.

7.1.2 Analysis Method

The method employed for the flaw stability analysis is the tearing instability analysis method using a J versus T diagram. The GE/EPRI elastic-plastic J estimation method (Reference 21), as modified by the improved J estimation scheme in EPRI report NP-4883M (Reference 22), is used for the evaluation of the circumferential through-wall flaws. This method superposes solutions corresponding to elastic and fully yielded conditions to obtain the elastic-plastic results for through-wall circumferential flaws in a cylinder subjected to combined tension and bending loads. The improved J-estimation formula is given as equation (7-11) in Section 7.3.1.2. The flaw stability calculations for the axial through-wall flaws are evaluated using the applied J and tearing modulus equations given in EPRI Ductile Fracture Handbook (Reference 23). For the evaluation of axial through-wall flaws, only the hoop stresses are significant. Therefore, only pressure is considered, because the hoop stresses due to the other loading constituents (axial load and bending moment) are negligible.

7.2 Analysis Procedure

The following procedure is used to evaluate the critical crack size considering the base and weld metal materials associated with the two selected LBB locations.

7.2.1 General

The flaw instability point can be determined by the J-T method described in Reference 1. The tearing modulus, T is defined as:

$$T = E/\sigma_f^2 \, dJ/da \qquad (7\text{-}1)$$

where E is Young's modulus and σ_f is the flow stress. For a stable crack growth the material's tearing modulus must be greater than the tearing modulus obtained from the applied load:

$$T_{applied} < T_{material} \qquad (7\text{-}2)$$

The instability point may be found by plotting $J_{applied}$ against $T_{applied}$ and $J_{material}$ versus $T_{material}$ on a single figure as illustrated by a plot showing J versus T in Figure 7-1. The intersection of the two curves is the instability point (point where $J_{applied} = J_{material}$) and the corresponding J value is $J_{instability}$ from which the maximum allowable moment can be determined.

7.2.2 J versus Applied Moment Diagrams

For a given applied loading on a pipe geometry with a through-wall flaw, $J_{applied}$ is calculated using the equations given in Section 7.3. As an example, J_{total} can be determined using Eq. (7-11) for an applied loading on a pipe geometry with a through-wall flaw size that is twice the leakage flaw size (for a 10 gpm leak rate) per S.R.P. 3.6.3. This equation is used to calculate $J_{elastic}$ and J_{total} for a family of applied moment loadings. The resulting J versus applied moment diagram is illustrated in Figure 7-2.

7.2.3 J-T Diagrams and Determination of $J_{upper\ limit}$

Using the applied J-integral equation, Eq. (7-11), J's are evaluated for small increments in crack size using the same set of applied moment loadings as discussed in Section 7.2.2. The tearing modulus is calculated by numerical differentiation of J as follows:

$$\frac{dJ}{da} = \frac{J(a+\zeta) - J(a-\zeta)}{2\zeta} \qquad (7\text{-}3)$$

where ζ is a small increment in crack size (0.01 inch is used in the analysis). Once the dJ/da calculations are performed, the tearing modulus calculations are readily performed using Eq. (7-1). The J-T analysis summaries are thereby created. Note that the material J-T curves are based on the power law formula of J-R data given in Section 3.3.3. The J-T diagram is then established as illustrated in Figure 7-1. From this figure, the $J_{instability}$ point can be determined. The $J_{instability}$ point is the intersection of the $J_{applied}$ and $J_{material}$ versus tearing modulus curves. At this point an alternate limit on J, called the $J_{upper\ limit}$ ($J_{U.L.}$), is introduced based on the maximum experimental J obtained from

an actual compact test specimen data. Whenever the applied J is limited by this J_{UL}, flaw stability is assured because $J_{instability}$ is greater than $J_{U.L.}$.

7.2.4 Summary of J-T Analysis Procedure

The applied J corresponding to the applied loading on the piping is compared with the material's J_{IC} and $J_{U.L.}$ values. Flaw stability is ensured if the applied J is less than J_{IC} or $J_{U.L.}$. The critical flaw size is then determined by incrementing the flaw size until the applied J corresponds to $J_{U.L.}$. The margin between the critical flaw size and the leakage flaw size (flaw size corresponding to a 10 gpm leak rate) is calculated and compared with the required margin of 2 per S.R.P. 3.6.3.

7.3 Flaw Stability Equations for Circumferential Flaws

7.3.1 Original Versus Improved J-estimation Scheme for Bending Loads

The flaw stability calculations are performed using J-integral estimation equations. The elastic-plastic J estimation formulae for the GE/EPRI estimation method are provided in EPRI report NP-3607 (Reference 16) and are updated in EPRI report NP-5596 (Reference 21). The J estimation formulae are given for circumferential through-wall flaws in a cylinder subjected to remote tension load and remote bending load as well as combined tension and bending loads.

The GE/EPRI method requires a Ramberg-Osgood representation of a stress-strain data in which the following expression is valid:

$$\varepsilon/\varepsilon_o = \sigma/\sigma_o + \alpha(\sigma/\sigma_o)^n \qquad (7\text{-}4)$$

where σ_o and ε_o are some reference stress and strain, n is the strain hardening constant, and α is a Ramberg-Osgood material constant.

The J integral estimation equation is of the form:

$$J(a,P) = J_e(a_e, P) + J_P(a, P) \qquad (7\text{-}5)$$

where J_e is the linear elastic component of the J-integral, and J_p is the plastic component of the J-integral.

For the case of a through-wall flaw in a pipe under remote bending, the GE/EPRI J estimation equation is given as:

$$J = J_e(a_{eff}) + \alpha\sigma_o\varepsilon_o c(a/b)h_1(M/M_o)^{n+1} \qquad (7\text{-}6)$$

where M_o is a reference limit moment determined using σ_o and c is half the uncracked portion of the pipe circumference. The circumferential through-wall flaw solutions are used to evaluate previously performed austenitic and ferritic steel pipe experiments

(References 24 and 25). The results from this evaluation (Reference 1) indicate that the J estimation scheme can be overly conservative for predicting initiation and maximum load. The conservatism in the calculated J at first extension varies by factors of 3 to 7 times the experimentally inferred values for the stainless steel pipe tests and by factors of up to 3 for the ferritic steel pipe tests (Reference 1).

The original GE/EPRI J integral estimation scheme is examined for possible modifications by Zahoor in EPRI report NP-4883M (Reference 22). In particular, the plastic portion of J is investigated carefully by Zahoor because the linear elastic solution is shown to agree with the results of other investigators. In References 16 and 26, the second term in the J formula comes from a finite element analysis using a pure power law material with $\alpha = 1$. It was assumed that J varies linearly with α; however, this assumption is not correct for the R-O type stress-strain curve.

The proposed improved GE/EPRI J-Integral estimation formula in EPRI report NP-4883M is:

$$J = J_e(a_{eff}) + \alpha^{1/(n+1)}\sigma_o\varepsilon_o c(a/b)h_1(M/M_o)^{n+1} \quad (7\text{-}7)$$

Examination of Eq. (7-7) indicates that the original plastic component of J is modified by replacing α with $\alpha^{1/(n+1)}$. This modification reduces the plastic J component compared to the original formulation. Predictions using the improved J-integral estimations are then compared against the pipe fracture data for both ferritic piping and stainless steel piping. The results indicate an accurate prediction for ferritic piping applications and reasonably good maximum load predictions for stainless steel pipes. As stated in EPRI report NP-4883M, the improved J estimation scheme removes the unwarranted conservatism found to exist in the original J estimation scheme.

Based on the above, the improved J estimation scheme, as given in EPRI report NP-4883M, is developed based on modifying the original GE/EPRI plastic component of J by replacing α with $\alpha^{1/(n+1)}$.

7.3.2 Improved EPRI/GE J estimation equation for Axial and Bending Loads

The GE/EPRI elastic-plastic J estimation method for determining the fracture parameters of a through-wall flaw in a cylinder subjected to combined tension and bending loads is described in Section 2.7.3 of Reference 21 and given in equation form below.

$$J = J_e(a_{eff})_P + J_e(a_{eff})_M + \alpha\sigma_o\varepsilon_o c(a/b)h_1(a/b, n, \lambda, R/t)\,[P/P_o']^{n+1} \quad (7\text{-}8)$$

where λ is the non-dimensional parameter that defines a relationship between the axial load, P, and the bending moment, M, in the following manner:

$$\lambda = M/PR \quad (7\text{-}9)$$

where R denotes the mean radius of the pipe. The first two terms of Eq. (7-8) represent the elastic part of the J-integral due to the axial load and the applied bending moment, respectively. The third term denotes the plastic part of the J-integral in which P_o' is the reference load for the combined tension and bending case:

$$P_{o'} = \frac{1}{2}\left[\frac{-\lambda P_o^2 R}{M_o} + \sqrt{\left(\frac{\lambda P_o^2 R}{M_o}\right)^2 + 4P_o^2}\right] \qquad (7\text{-}10)$$

where:

$P_o = 2\sigma_o Rt(\pi - \gamma - 2\arcsin(0.5\sin\gamma))$
$Mo = M_o'(\cos(\gamma/2) - 0.5\sin(\gamma))$
$M_o' = 4\sigma_o R^2 t$
$\gamma = a/R$

As discussed in Section 7.3.1 and proposed in Reference 22, the improved J estimation scheme is obtained by replacing the α in the original GE/EPRI plastic component of J with $\alpha^{1/(n+1)}$. Incorporating this modification to Eq. (7-8) results in the improved J-estimation formula as given below.

$$J = J_e(a_{eff})_P + J_e(a_{eff})_M + \alpha^{1/(n+1)}\sigma_o\varepsilon_o c(a/b)h_1(a/b, n, \lambda, R/t)\,[P/P_o']^{n+1} \qquad (7\text{-}11)$$

The above formula is used in the flaw stability analysis of the circumferential through-wall flaws. The resulting J versus applied moment diagram and J versus T diagram for LBB location 1 with base metal properties are illustrated in Figures 7-3 and 7-4, respectively. The J versus T diagram for LBB location 1 using weld metal properties is given in Figure 7-5. Similarly, the J versus T diagrams for LBB location 2 with applicable base and weld metal properties are illustrated in Figures 7-6 through 7-8.

7.4 Flaw Stability Equations for Axial Flaws

As stated in Section 7.1.2, the axial through-wall flaws were evaluated using the applied J and tearing modulus equations given in EPRI Ductile Fracture Handbook (Reference 23). The applied J and tearing modulus equations due to internal pressure are given below.

$$J = (8c\sigma_f^2/\pi E) \cdot \ln[\sec(M\pi\sigma/2\sigma_f)] \qquad (7\text{-}12)$$

where

$M = [1 + 1.2987\lambda^2 - 0.026905\lambda^4 + 5.3549\times10^{-4}\lambda^6]^{0.5}$
$\lambda = c/(Rt)^{0.5}$
$\sigma = pR/t$
σ_f = flow stress

$$T_a = (J/c) \cdot (E/\sigma_f^2) + H_o(\sigma/\sigma_f) \cdot \tan(M\pi\sigma/2\sigma_f) \quad (7\text{-}13)$$

where

$T_a = (\partial J/\partial c)_p E/\sigma_f^2$

J and M = as defined above in the J integral equation

$H_o = 4[1.2987\lambda^2 - 0.05381\lambda^4 + 1.60645 \times 10^{-3}\lambda^6] / M$

λ, σ and σ_f = as defined above in the J integral equation

7.5 Summary of Results

The results from the flaw stability analysis of circumferential and axial through-wall flaws at the two critical locations in the CF and LPI/DHR piping systems are summarized in Tables 7-1 and 7-2 respectively. The leakage flaw size (one-half the leakage size crack length) are also given in these tabulations. The two critical locations are: (1) core flood piping attached to the bottom of the core flood tank nozzle and (2) reactor vessel core flood nozzle safe-end to pipe juncture. The results given in Tables 7-1 and 7-2 clearly show that the circumferential through-wall flaws provide the more limiting margin on flaw size. The results of the circumferential through-wall flaws at the two locations are discussed below (Reference 12).

7.5.1 Core Flood Piping Attached to the Bottom of the Core Flood Tank Nozzle

The limiting material for this region of the piping is determined to be the Type 304 stainless steel base metal. The maximum applied value of J is determined to be 2.834 kips/in which is less than the J_{IC} of the material (5.04 kips/in). The critical flaw size is determined to be 8.00 inches and the margin on flaw size is determined to be 2.5.

7.5.2 Reactor Vessel Core Flood Nozzle Safe-End to Pipe Juncture

The limiting material for this region of the piping is also determined to be the Type 304 stainless steel base metal. The maximum applied value of J is determined to be 1.071 kips/in which is less than the J_{IC} of the material (4.58 kips/in). The critical flaw size is determined to be 8.87 inches and the margin on flaw size is calculated to be 2.6.

Table 7-1. Summary of Results for Circumferential Flaws

Piping Location[1]	Material[2]	Leakage Flaw Size[3], a (in)	$J_{applied}$[4] (kips/in)	Material J_{IC}[5] (kips/in)	Instability Criteria $J_{U.L.}$[6] (kips/in)	Critical Flaw Size[7] a_c (in)	Margin on Flaw Size[8]
1	Type 304SS Base	3.21	2.834	5.04	10.0	8.00	2.5
	GTAW Weld	3.21	1.203	3.2	10.0	9.70	3.0
2	SMAW Weld	3.435	0.286	0.994	2.5	9.74	2.8
	Type 316SS Base	3.435	0.304	4.05	10.0	9.52	2.8
	Type 304SS Base	3.435	1.071	4.58	7.0	8.87	2.6

[1] Location 1 refers to core flood piping attached to bottom of the core flood tank nozzle.
Location 2 refers to reactor vessel core flood nozzle safe-end to pipe juncture.

[2] General description of base metal or weld metal considered in the analysis

[3] Corresponds to one-half of the leakage crack length as predicted by KRAKFLO in Reference 19.

[4] Due to applied moment loading (using the absolute load combination method) with a factor of two on the leakage flaw size.

[5] From deformation J-R curve for the material

[6] A value less than $J_{instability}$. $J_{U.L.}$ is based on a maximum crack extension from an actual compact test specimen data.

[7] Maximum allowable flaw size that ensures stability of the flaw for the given applied loading.

[8] Critical flaw size divided by the leakage flaw size.

Table 7-2. Summary of Results for Axial Flaws

Piping Location[1]	Material[2]	Leakage Flaw Size[3], a (in)	$J_{applied}$[4] (kips/in)	Material J_{IC}[5] (kips/in)	Instability Criteria $J_{U.L.}$[6] (kips/in)	Critical Flaw Size[7] a_c (in)	Margin on Flaw Size[8]
1	Type 304SS Base	2.195	0.64	5.04	10.0	7.99	3.6
	GTAW Weld	2.195	0.60	3.2	10.0	7.99	3.6
2	SMAW Weld	2.555	0.42	0.994	2.5	9.50	3.7
	Type 316SS Base	2.555	0.43	4.05	10.0	12.76	5.0
	Type 304SS Base	2.555	0.46	4.58	7.0	10.09	3.9

[1] Location 1 refers to core flood piping attached to bottom of the core flood tank nozzle.
Location 2 refers to reactor vessel core flood nozzle safe-end to pipe juncture.

[2] General description of base metal or weld metal considered in the analysis

[3] Corresponds to one-half of the leakage crack length as predicted by KRAKFLO in Reference 19.

[4] Due to applied pressure loading at steady state condition with a factor of two on the leakage flaw size.

[5] From deformation J-R curve for the material

[6] A value less than $J_{instability}$. $J_{U.L.}$ is based on a maximum crack extension from an actual compact test specimen data.

[7] Maximum allowable flaw size that ensures stability of the flaw for the given applied loading.

[8] Critical flaw size divided by the leakage flaw size.

Figure 7-1 Illustration of the Stability Assessment Point

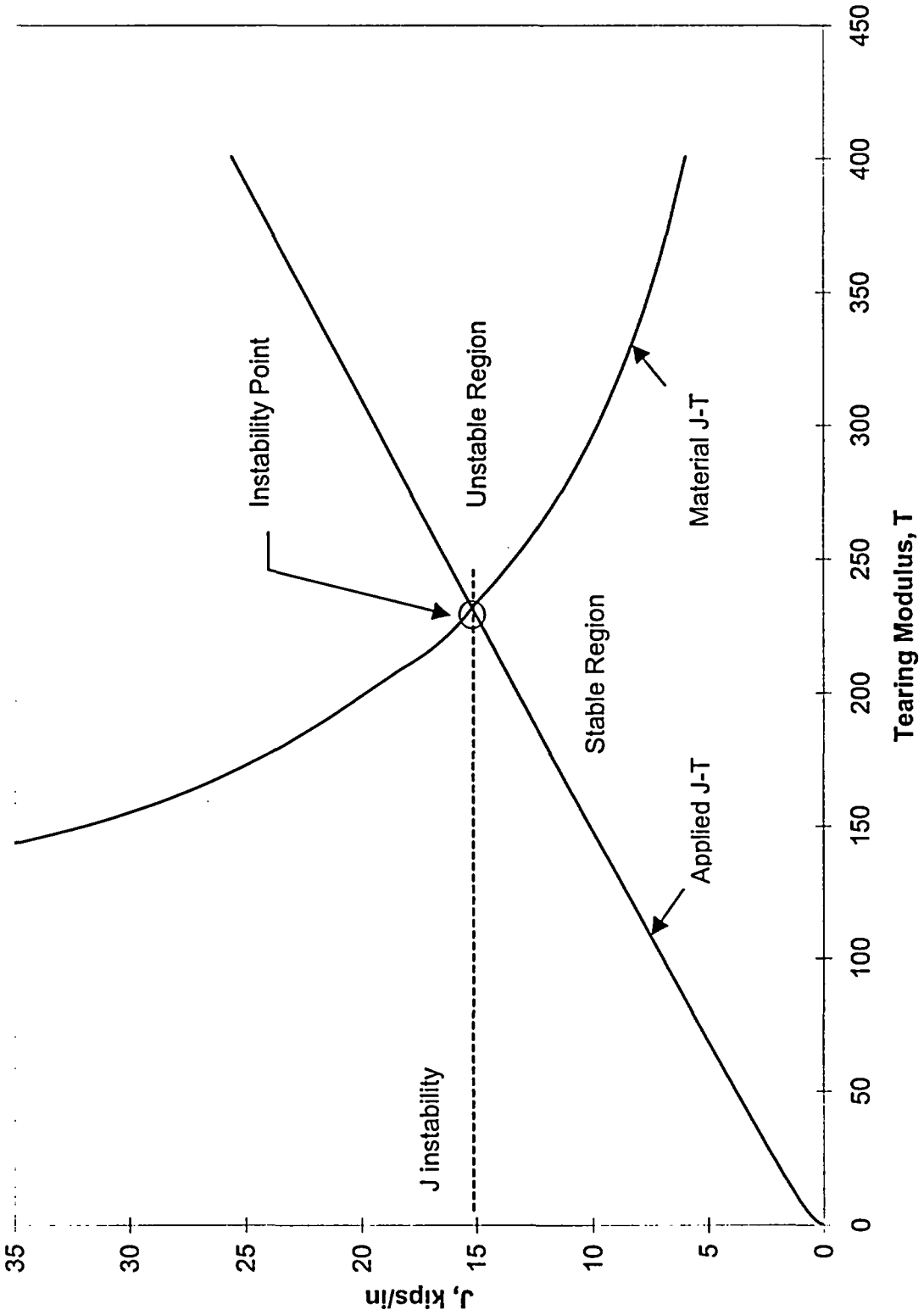

AREVA

Figure 7-2 Illustration of J versus Applied Moment Loading Diagram

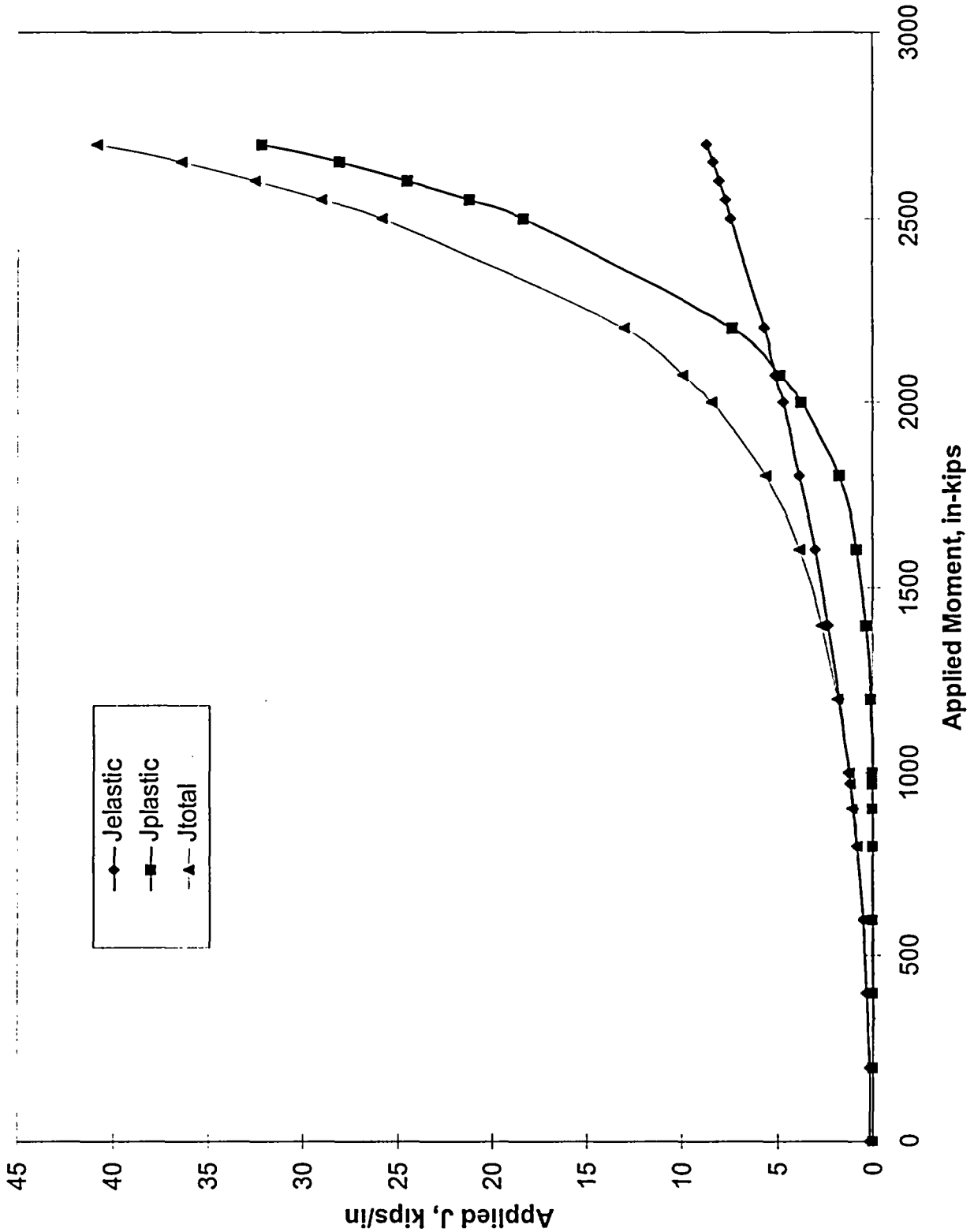

AREVA

Figure 7-3 Applied J versus Moment Diagram for Type 304SS Base Metal at LBB Location 1

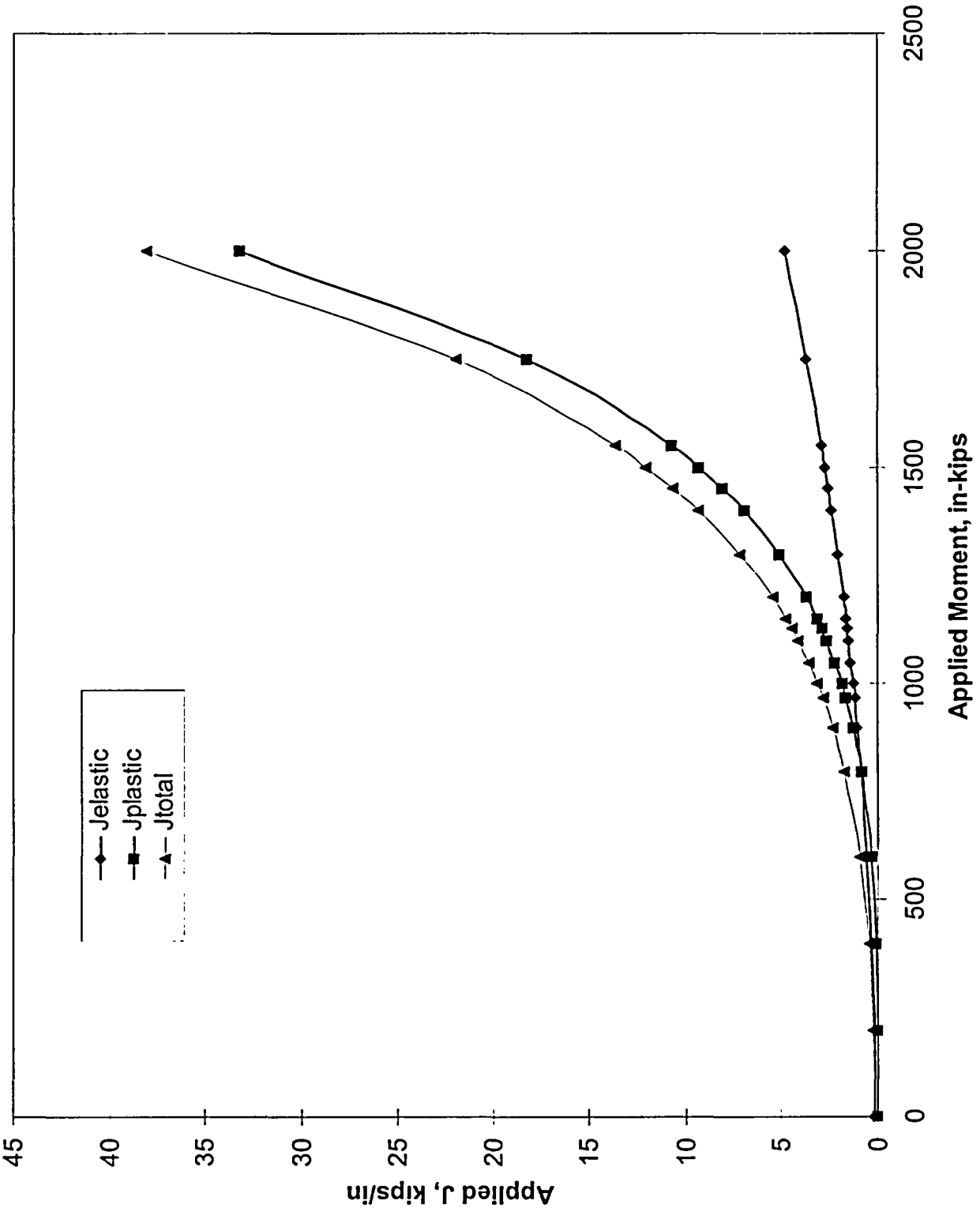

AREVA

Figure 7-4 J versus T diagram for Type 304SS Base Metal at LBB Location 1

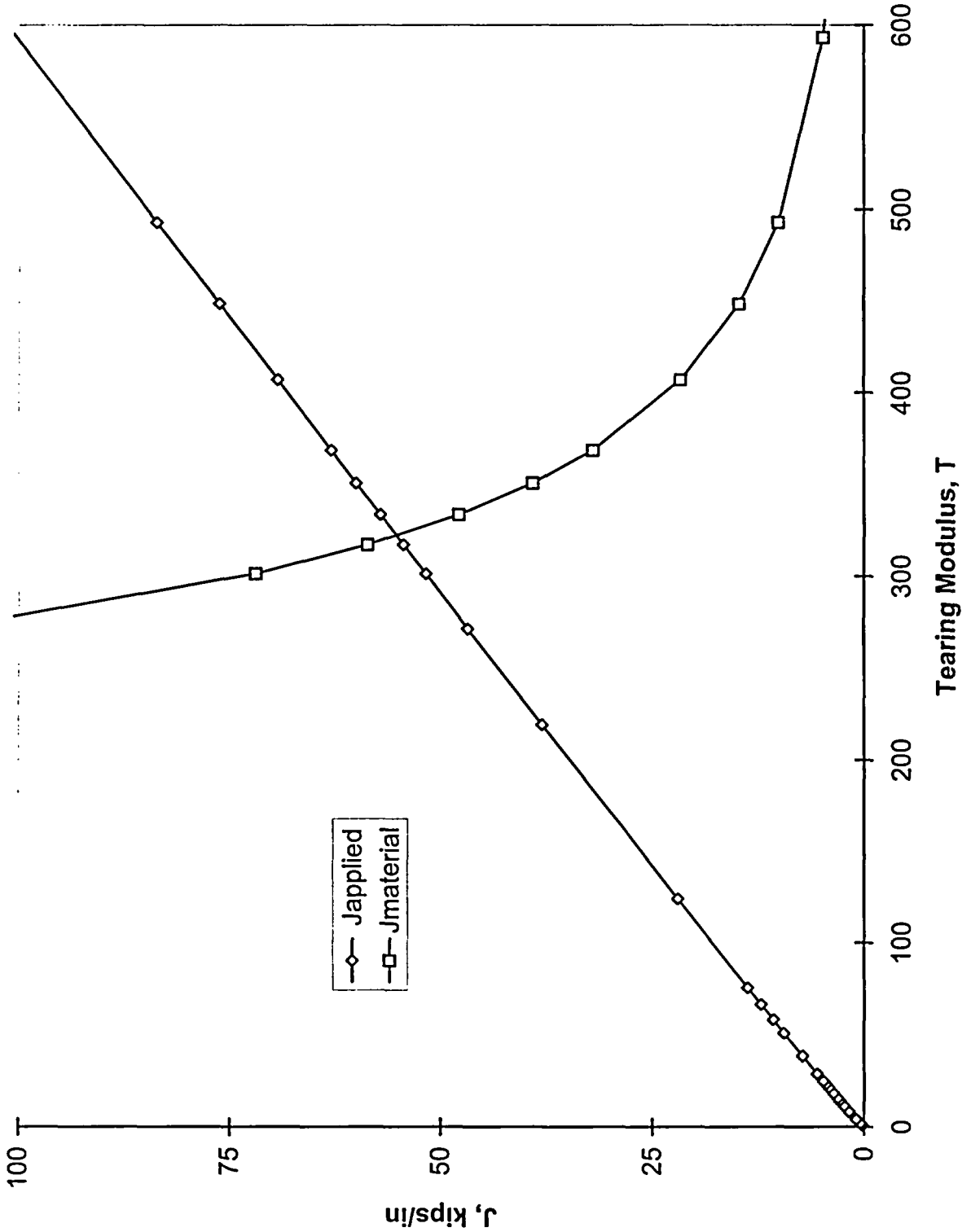

AREVA

Figure 7-5 J versus T diagram for GTAW Weld Metal at LBB Location 1

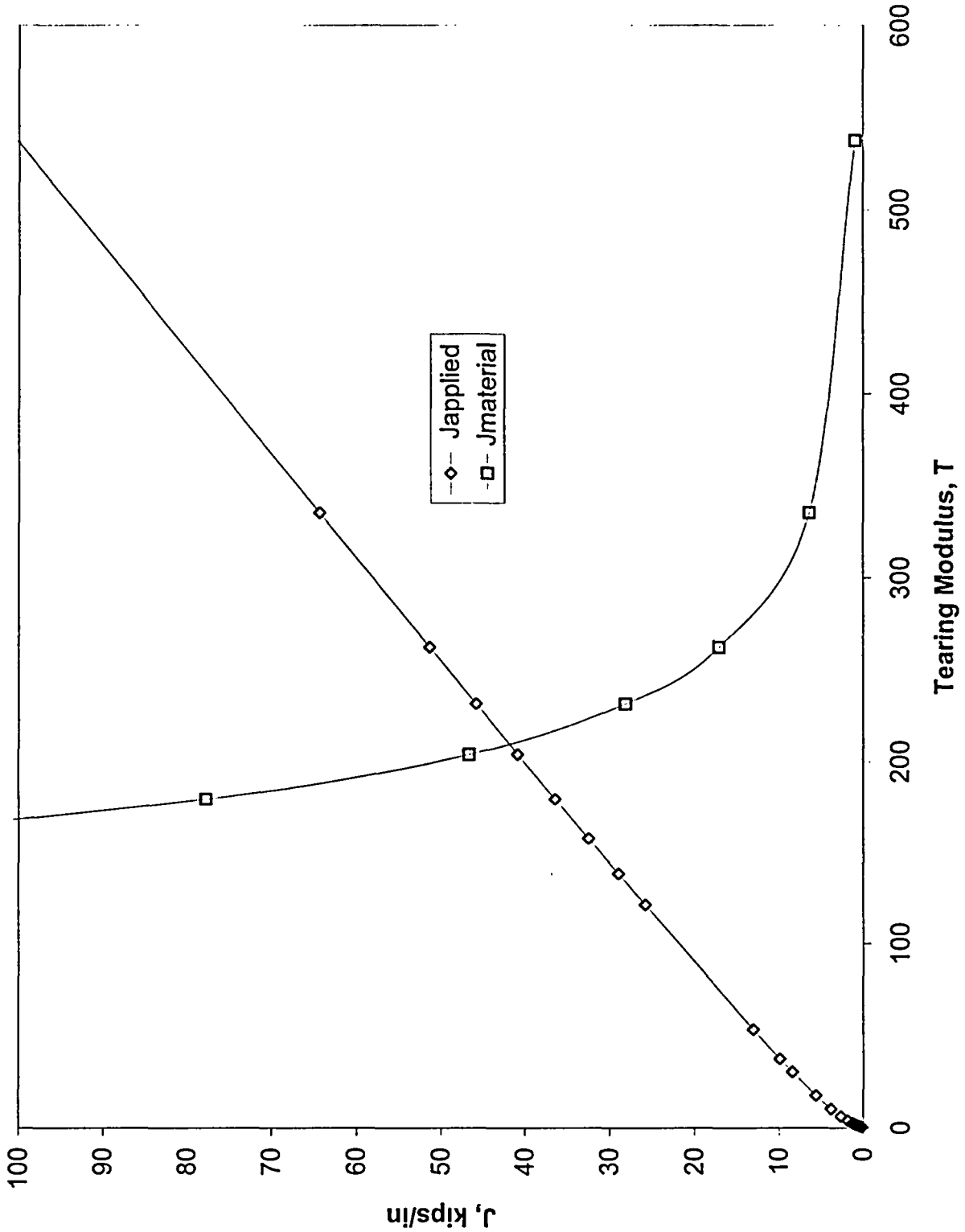

AREVA

Figure 7-6 J versus T diagram for Type 316SS Base Metal at LBB Location 2

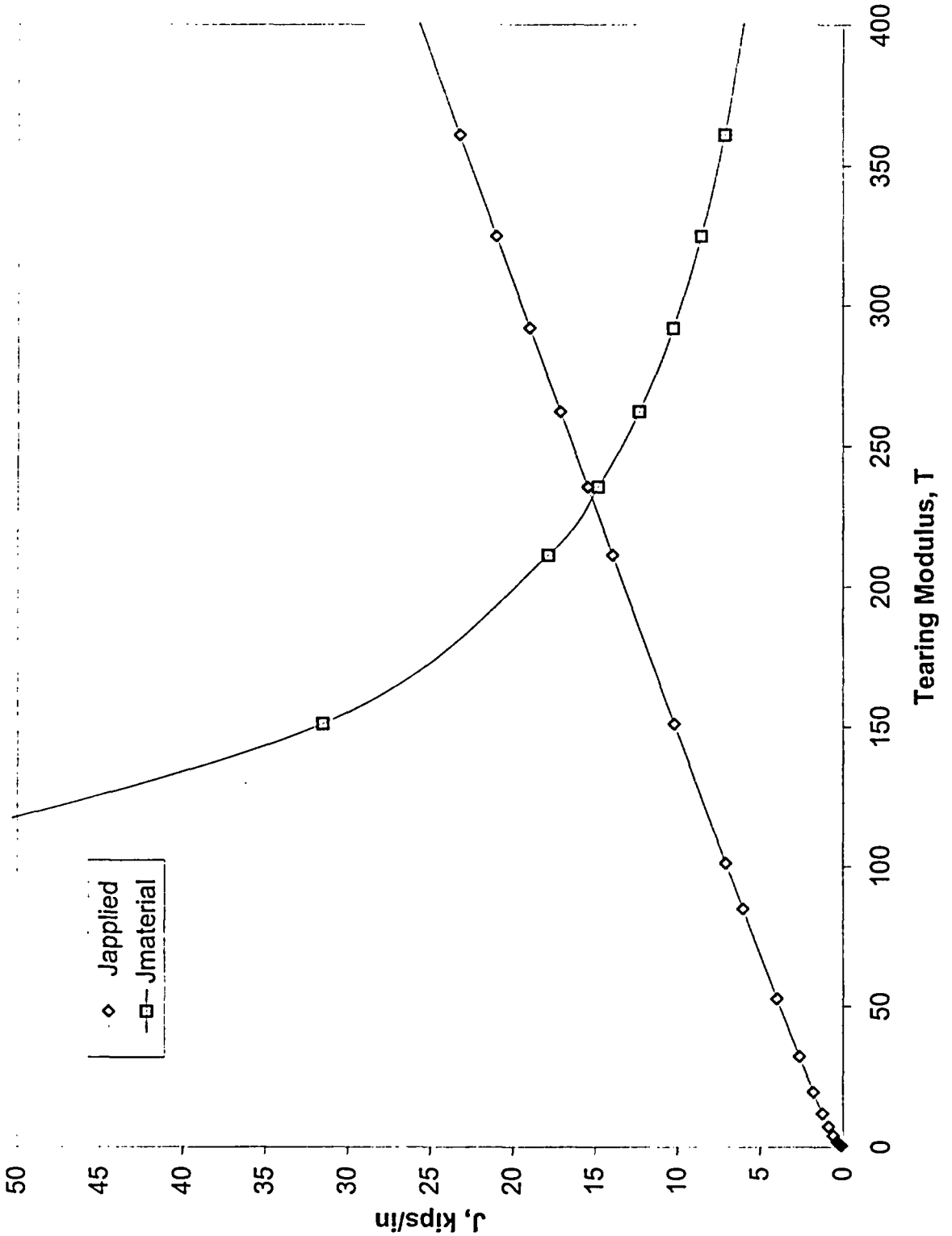

AREVA

Figure 7-7 J versus T diagram for Type 304SS Base Metal at LBB Location 2

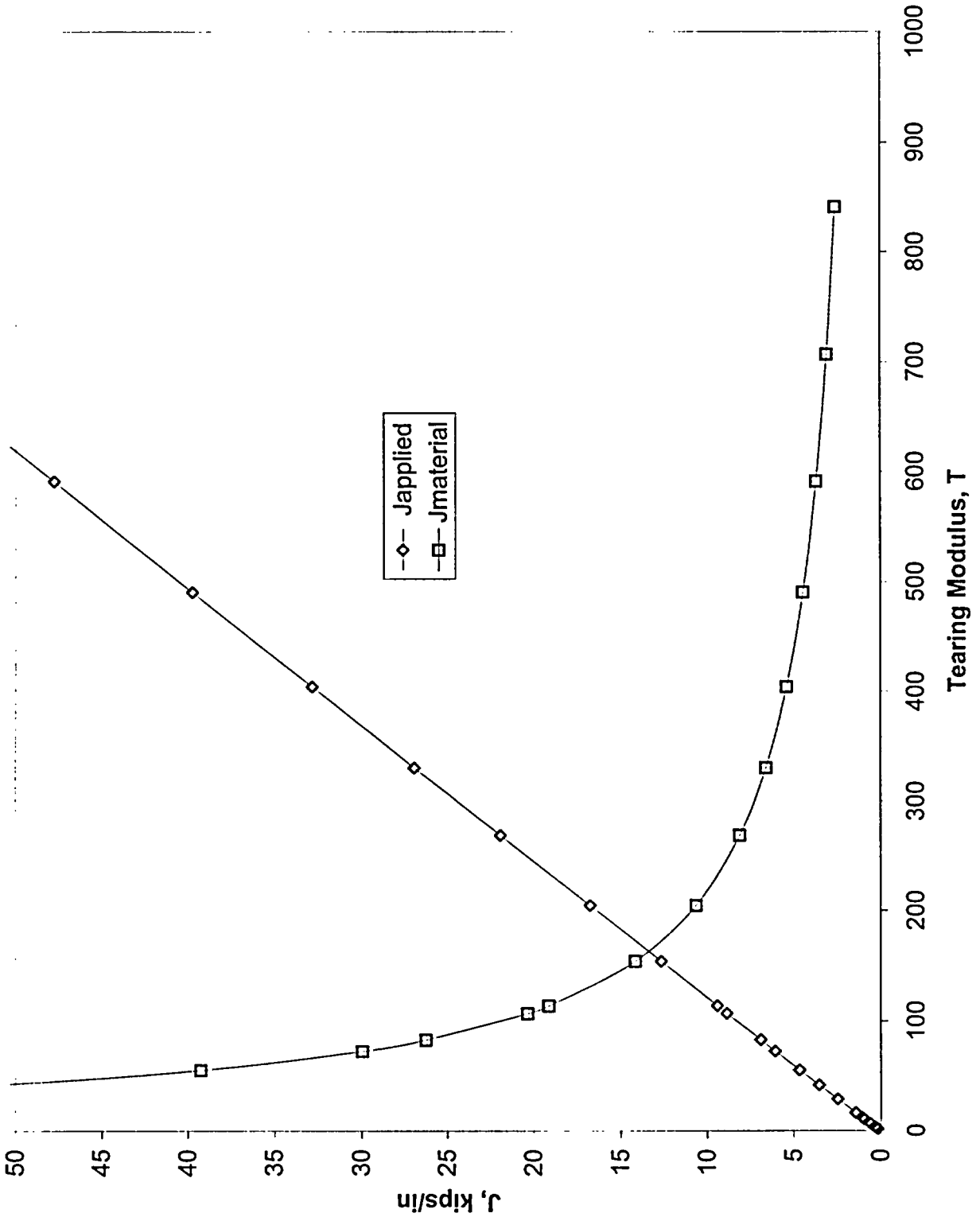

AREVA

Figure 7-8 J versus T diagram for SMAW Weld Metal at LBB Location 2

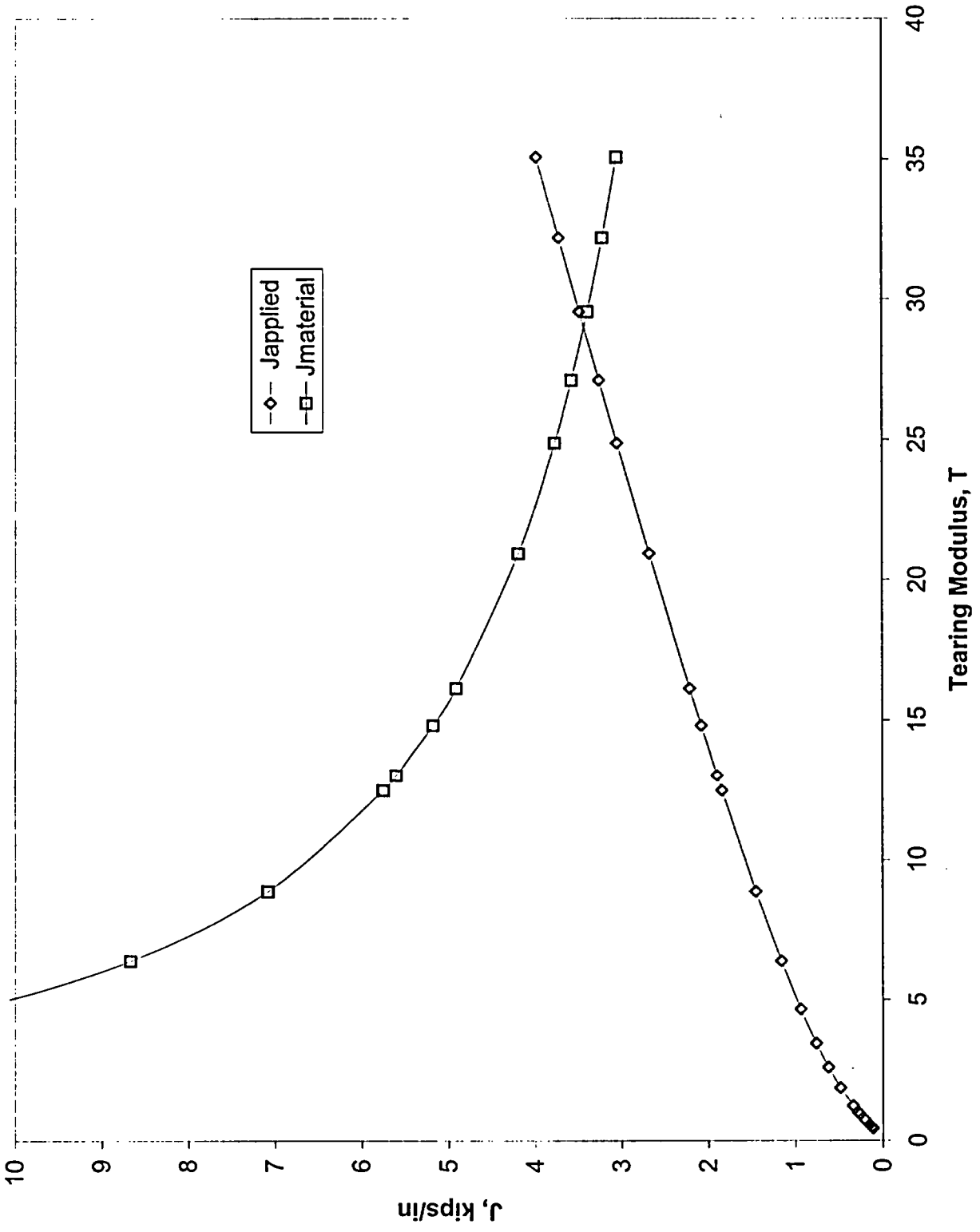

AREVA

8. CONCLUSION

This report demonstrates that leak-before-break technology is applicable to the CF and applicable portion of LPI/DHR piping system of Oconee Unit 3. The piping systems included in the scope of this report are the 14 inch CF line connecting the core flood tank with the reactor vessel (train "A" & train "B"), and the high-energy section of the 10 inch LPI/DHR line that will connect the check valve to the core flood line (planned modification for Fall 2004). Due to PWSCC issues, the Alloy 82/182 bi-metallic weld between the core flood nozzle of the RV and the safe-end piping (both locations) are excluded from this LBB evaluation. However, the Alloy 82/182 bi-metallic welds at the A & B Core Flood Tanks are included since PWSCC concerns are not applicable at these locations due to low operating temperatures.

General Design Criterion 4 of 10 CFR 50, S.R.P. 3.6.3, and NUREG-1061 provide limitations to be applied to the mechanistic evaluation of pipe breaks in high-energy fluid system piping. The CF and LPI/DHR piping within the scope of this report meets all of those limitations.

Based on identification of locations with the least favorable combinations of high stress and poor material properties, the critical locations for LBB analysis are identified as:

Location 1: Core Flood Piping Attached to Bottom of the Core Flood Tank Nozzle
Location 2: Reactor Vessel Core Flood Nozzle Safe-End to Pipe Juncture

Based on the design and operational standards for the leakage detection equipment inside containment, a leakage rate of 1 gpm is identifiable for the Oconee CF and LPI/DHR systems. Proposed S.R.P 3.6.3 requires a margin of 10 on the detectable leak rate. Therefore, a leakage rate of 10 gpm is used for the LBB analysis of this report.

The leakage size crack (LSC) is defined as the crack size allowing a 10 gpm leak rate. The LSC lengths for the two critical locations analyzed in this report are:

Location 1: Circumferential LSC = 6.42 inches, Longitudinal LSC = 4.39 inches
Location 2: Circumferential LSC = 6.87 inches, Longitudinal LSC = 5.11 inches

The flaw stability analysis of the CF and LPI/DHR piping systems of Oconee Unit 3 meets all of the safety margin requirements of S.R.P. 3.6.3. The most limiting location and material for LBB analysis is determined to be the piping adjacent to the core flood tank nozzle (Location 1) and Type 304 stainless steel base metal material, respectively. Considering a factor of two on the 10 gpm leakage flaw size, the maximum applied J (due to maximum moment loading using the absolute load combination method) is determined to be 2.834 kips/in. The stability of the flaw is ensured since it is less than

the J_{IC} value of the material (5.04 kips/in). The margin on flaw size is determined to be 2.5 which is greater than the required margin of 2.

Based on these analyses and system reviews, it is concluded that the application of leak-before-break technology to the CF and LPI/DHR piping systems within the scope of this report is justified.

9. REFERENCES

1. NUREG-1061, Volume 3, "Report of the U.S. NRC Piping Review Committee - Evaluation of Potential for Pipe Breaks," US NRC, 10/84.

2. Standard Review Plan 3.6.3, Federal Register Volume 52, Number 167, 8/87.

3. Code of Federal Regulations, 10 CFR Part 50, Appendix A, US Government, 11/88.

4. NUREG-0582, "Water Hammer in Nuclear Power Plants," US NRC, 7/79.

5. NUREG/CR-2781, "Evaluation of Water Hammer Events in Light Water Reactor Plants," US NRC, 7/82.

6. NUREG-0927, "Evaluation of Water Hammer Occurrence in Nuclear Power Plants," Rev. 1, US NRC, 3/84.

7. FANP Document No. 51-1212842-00, "Oconee Stratif. Data - 6/90 HU."

8. EPRI Report TR-103844s, "PWR Reactor Coolant System License Renewal Industry Report; Revision 1," 7/94.

9. Oconee Nuclear Station Final Safety Analysis Report, December 1996 Revision.

10. ASME Boiler and Pressure Vessel Code, Section III, Division 1 - Appendices, 1989 Edition.

11. EPRI Report NP-4768, "Toughness of Austenitic Stainless Steel Pipe Welds," Westinghouse Electric Corporation, 10/86.

12. FANP Document 32-1258816-01, "FM Analysis for LBB of Oconee CFL" (FANP Proprietary).

13. FANP Document 32-1258655-04, "DPC CFL LBB Leak Rate Analysis" (FANP Proprietary).

14. BAW-2243A, "Demonstration of the Management of Aging Effects for the Reactor Coolant System Piping," 6/96.

15. US Nuclear Regulatory Guide 1.45, "Reactor Coolant Pressure Boundary Leakage Detection Systems," 5/73.

16. EPRI Report NP-3607, "Advances in Elastic-Plastic Fracture Analysis," 8/84.

17. NUREG/CR-3464, "The Application of Fracture Proof Design Methods Using Tearing Instability Theory to Nuclear Piping Postulating Through Wall Cracks," US NRC, P.C. Paris and H. Tada, 9/83.

18. USA Standard B31.7, "Nuclear Power Piping," 1968 Edition, including errata of June 1968.

19. FANP Manual No. UPGD-TM-38, KRAKFLO User's Manual, "Fortran Program for Calculating Flow Through Narrow Cracks," Rev. E, 5/96.

20. EPRI Report NP-3395, "Calculation of Leak Rates Through Cracks in Pipes and Tubes," 1983.

21. EPRI Report NP-5596, "Elastic-Plastic Fracture Analysis of Through-Wall and Surface Flaws in Cylinders," 1/88.

22. EPRI Report NP-4883M, "Evaluation of Flawed-Pipe Experiments," 11/86.

23. EPRI Report NP-6301-D, Volume 2, Chapter 6, "Ductile Fracture Handbook," 10/90.

24. EPRI Report NP-2347, Vol. 1 and 2, "Instability Predictions for Circumferentially Cracked Type 304 Stainless Steel Pipe Under Dynamic Loading," 4/82.

25. NUREG/CR-3740, "J-Integral Tearing Instability Analysis for 8-inch Diameter ASTM A 106 Steel Pipe," 4/84.

26. M.D. German and V. Kumar, "Elastic-Plastic Analysis of Crack Opening, Stable Growth and Instability Behavior in Flawed 304 Stainless Steel Piping," ASME PVP Vol. 58, American Society of Mechanical Engineers, 7/82.